

# Structural behaviour of stud shear connections in composite floors with various connector arrangements and profiled deck configurations

Min-hui Shen <sup>a</sup>, Kwok-Fai Chung <sup>\*b,c</sup>, Ahmed Y. Elghazouli <sup>d</sup>, and Jing-Zhong Tong <sup>e</sup>

<sup>a</sup> Department of Urban Construction and Safety Engineering,  
Shanghai Institute of Technology, China.

<sup>b</sup> Department of Civil and Environmental Engineering,  
the Hong Kong Polytechnic University, Hong Kong SAR, China.

<sup>c</sup> Chinese National Engineering Research Centre for Steel Construction (Hong Kong Branch),  
the Hong Kong Polytechnic University, Hong Kong SAR, China.

<sup>d</sup> Department of Civil and Environmental Engineering, Imperial College London, UK.

<sup>e</sup> College of Civil Engineering and Architecture, Zhejiang University, Hangzhou, China.

## Abstract

This paper investigates the structural behaviour of stud shear connections in composite floors with various connector arrangements and profiled deck configurations. The numerical investigation adopts a number of advanced finite element models which have been carefully calibrated against standard push-out tests conducted by the authors. In order to capture the complex interactions that take place between the concrete and the headed shear studs, a number of distinctive load transfer mechanisms within the solid concrete and the profiled composite slabs are identified and discussed. Detailed parametric studies are then undertaken using the calibrated models for the purpose of quantifying the shear resistance and deformation characteristics for connections with various stud and deck arrangements. A configuration parameter  $\beta$  is proposed for use in conjunction with the reduction factor  $k_t$  given in EN 1994-1-1 to incorporate the effects of installation positions of headed shear studs and trough widths of profiled decks as well as the presence of longitudinal stiffeners if any. It is shown that the values of  $\beta$  are in the range of 0.55 to 1.0, which are significantly smaller than those commonly allowed for in the design of stud shear connections in composite floors.

## Keywords:

Stud shear connections; finite element modelling; load transfer mechanisms; load-slippage curves; shear resistances.

---

\* Corresponding author: [kwok-fai.chung@polyu.edu.hk](mailto:kwok-fai.chung@polyu.edu.hk)

## 44 **1. Introduction**

45 In composite members, stud shear connectors of various forms are used to transmit longitudinal  
46 shear forces at the steel-concrete interfaces. The structural behaviour of these connectors has a  
47 direct influence on the effectiveness of the composite members in acting as integral members  
48 in resisting the applied loads. The most widely used shear connectors in building construction  
49 are headed shear studs, typically with a diameter of 19 mm, a height of 100 mm, and a tensile  
50 strength of 450 N/mm<sup>2</sup>. Deformation characteristics of these stud shear connections in solid  
51 and composite slabs are commonly determined from push-out tests shown in Figure 1.

52

53 According to previous experimental investigations [1-3], numerical assessments [4-11], and  
54 theoretical studies [12, 13], the shear resistance of a stud shear connection in a composite beam  
55 with a profiled deck largely depends on the following factors:

- 56 a) concrete compressive and tensile strengths as well as elastic modulus;
- 57 b) tensile strength of headed shear studs as well as their shapes and sizes;
- 58 c) welding quality of shear studs and dimensions of welding collars at stud roots;
- 59 d) arrangements of headed shear studs within the troughs of profiled decks including position  
60 and spacing;
- 61 e) yield and tensile strengths of profiled decks and their cross-sectional shapes and  
62 dimensions, as well as sizes of longitudinal stiffeners in deck troughs, if present;
- 63 f) spanning direction of profiled decks, if present;
- 64 g) sizes and arrangement of steel reinforcement in the vicinity of the shear studs.

65

### 66 1.1 Recent experimental and numerical studies

67 Work carried out over the past decade have raised some concerns regarding the ductility of  
68 some forms of the stud shear connections for which considerable resistance degradation tend  
69 to occur at relatively small slippages [14]. However, in composite beams incorporating such  
70 shear connections, there was no apparent adverse effect on the overall beam behaviour, and  
71 their load-deflection curves were often shown to be sufficiently ductile [15]. Hence, there  
72 was a significant discrepancy in the deformation characteristics of these shear connections, as  
73 determined from push-out tests, when compared with those measured in beam tests. More

74 recently, several researchers have also examined the shear resistances of these shear  
75 connections under combined shear and tension forces [16-18], as well as even under cyclic  
76 loading [19, 20]. In general, owing to the large number of factors that affect the structural  
77 behaviour of these stud shear connections, significant variations are often observed in the test  
78 results obtained from various push-out tests. It is therefore vital to select test results from only  
79 those experimental investigations which have been carefully and consistently executed, and  
80 which material data and test results have been presented in a systematic manner.

81

82 In recent years, several researchers have also investigated the fundamental behaviour of stud  
83 shear connections through advanced finite element modelling. Katwal et al [10] established a  
84 finite element model of a composite beam with a profiled deck by detailed modelling of the  
85 interaction between the steel beam and the composite slab. The stud shear force-slippage curves  
86 of the shear connections were obtained, and one of the key areas of investigation was to assess  
87 contributions of the profiled deck to the shear resistance of the connections. Vigneri et al. [11]  
88 also performed numerical simulations to identify various development stages of plastic hinges  
89 along the shanks of the headed shear studs. It is expected that such deformation characteristics  
90 would be more complex in composite beams with various connector arrangements and profiled  
91 deck configurations.

92

## 93 1.2 Experimental and numerical investigations by the authors

94 In order to assess and quantify the structural behaviour of stud shear connections in composite  
95 beams, an experimental assessment coupled with complementary numerical simulations was  
96 carried out previously by the authors [18, 21].

97

### 98 1.2.1 Systematic standard push-out tests

99 A total of three series of push-out tests comprising a total of 13 tests were undertaken to obtain  
100 the load-slippage curves of stud shear connections with different configurations, as shown in  
101 Figure 1:

102 • Test Series SS

103 In this series, standard push-out tests were performed on stud shear connections with  
104 concrete solid slabs. Four pairs of headed shear studs were installed in each test specimen,  
105 and were fully embedded into the concrete. Both the measured load-slippage curves and  
106 the measured shear resistances of the test specimens are adopted as the reference data of  
107 the shear connections for subsequent comparisons.

108 • Test Series SCFr and SCUr

109 In these two series, standard push-out tests were performed on shear connections in  
110 composite slabs. Four pairs of headed shear studs were employed in each test specimen,  
111 and were installed in either a “favourable” or an “unfavourable” position in the troughs of  
112 the profiled decks, owing to the presence of longitudinal stiffeners.

113

114 Among these tests, all specimens with solid concrete slabs failed through stud fracture while  
115 all specimens with composite slabs failed in concrete conical failure, as shown in Figure 2. The  
116 measured load-slippage curves were normalized through a linear reduction factor which is a  
117 ratio of the reference strength of 35 N/mm<sup>2</sup> to the measured compressive strength of the  
118 concrete, or of the reference strength of 500 N/mm<sup>2</sup> to the measured yield strength of the steel  
119 studs, depending on the modes of failure of the test specimens. Details of the material tests of  
120 both the concrete and the steel studs may be found in Shen [22].

121

122 Representative load-slippage curves of these shear connections with different configurations  
123 are plotted together for direct comparison, as shown in Figure 3, and the measured shear  
124 resistances per stud are summarized in Table 1 for ease of comparison. Based on the results of  
125 the push-out tests, a set of reduction factors allowing for the presence of the profiled decks as  
126 well as for different stud arrangements in the deck troughs have were obtained. It was found  
127 that the design rules for  $k_t$  given in EN 1994-1-1 [23] and BS 5950-3 [24] are inadequate for  
128 cases of headed shear studs installed in both the favourable and the unfavourable positions of  
129 the deck troughs.

130 It should be noted that a number of tensile tests were conducted on the coupons machined from  
131 the headed shear studs according to EN ISO 6892-1:2009 [25], and key mechanical properties  
132 obtained from measured engineering stress-strain curves of these studs were adopted for  
133 subsequent numerical analyses.

134

### 135 1.2.2 Development of advanced numerical models

136 Using detailed finite element procedures, material models and solution techniques [4-11],  
137 numerical simulations were carried out by the authors [21] to replicate the push-out tests  
138 described above. Element type C3D8R in ABAQUS [26] was used to model the concrete slab,  
139 the steel section and the headed shear studs while element S4R was adopted to model the deck.  
140 For the steel reinforcement, a two-noded linear three-dimensional truss element T3D2 was  
141 employed.

142

143 Key information of the finite element modelling technique is reported as follows.

#### 144 a) Material model of stud steels

145 According to test results of standard tensile tests, the material model of the stud steels is  
146 represented with a non-linear true stress-strain relationship transformed by integration method  
147 based on the minimum engineering stress-strain curve. The deformation limit of true strain is  
148 specified as 5%. The transformation rules are:

$$149 \quad \varepsilon_t = \ln ( 1 + \varepsilon ) \quad ; \text{ and}$$

$$150 \quad \sigma_t = \sigma ( 1 + \varepsilon )$$

151 where

152  $\sigma$  and  $\varepsilon$  are the engineering stress and strain, respectively, and

153  $\sigma_t$  and  $\varepsilon_t$  are the true stress and strain, respectively.

154 Since the objective of the present study is to investigate the load-transfer mechanisms of the  
155 shear connections, the deformation limit of 5% in the shear studs defined in the material model  
156 is considered to be sufficient to identify all possible failure modes in the shear connections.

157

158 b) Material models of concrete

159 For the concrete material, the concrete damaged plasticity (CDP) model [27-29] is adopted  
160 which involves two main failure mechanisms, namely, i) compressive crushing, and ii) tensile  
161 cracking. In general, this model assumes that the uni-axial compressive and tensile response  
162 of the concrete is characterized by damaged plasticity, and this simplified representation is able  
163 to capture main features of the mechanical responses of the concrete readily. The yield function  
164 of this model is proposed by Lubliner et al. [28], and then subsequently modified by Lee et al.  
165 [29]. In the present numerical investigation, the following values of the plasticity parameters  
166 of the concrete are adopted for the CDP model in ABAQUS [26]:

167

- 168 i)  $\Psi$  is the dilation angle measured on the p-q plane at high confining pressures, and it  
169 is taken to be  $40^\circ$ ;
- 170 ii)  $M$  is a parameter that defines the rate at which the function approaches the  
171 asymptote, and it is taken to 0.1;
- 172 iii)  $f_{b0}/f_{c0}$  is a ratio of the initial bi-axial compressive yield stress to the initial uni-axial  
173 compressive yield stress, and it is taken as 1.16;
- 174 iv)  $K_c$  is a ratio of the second stress invariant on the tensile meridian,  $q(TM)$ , to that  
175 on the compressive meridian,  $q(CM)$ ; and it is taken to be 0.667;

176

177 The viscosity parameter is taken to be zero so that no visco-plastic regularization is performed.  
178 For further details on the values of those parameters, refer to Qureshi et al. [5]. In general, the  
179 model is shown to give good predictions when the concrete is under uni-axial and bi-axial stress  
180 states. It should also be noted that:

- 181 • under uni-axial compression, the stress-strain relationship provided by EN 1992-1-1 [30]  
182 and the elastic modulus of the concrete given in the Hong Kong Concrete Code [31] are  
183 adopted; and
- 184 • under uni-axial tension, the tensile behaviour of the concrete is interpreted as the  
185 relationship between the tensile stress and the cracking displacement given in both EN  
186 1992-1-1 [30] and fib Model Code 2010 [32].

187

188 It should be noted that a new CDP model with mesh-insensitivity proposed by Alfarah et al [27]  
189 is reported to be very effective in modelling concrete cracking, concrete crushing, and  
190 reinforcement steel yielding in typical reinforced concrete members under both monotonic and

191 cyclic actions.

192

193 a) Contact models

194 In order to model the surface-to-surface contact in the shear connections properly, the following  
195 four models of contact pairs are set up:

196 i) the steel section onto the concrete slab,

197 ii) the headed shear stud onto the concrete,

198 iii) the top surface of the profiled deck onto the concrete, and

199 iv) the bottom surface of the profiled deck onto the steel sections.

200

201 In general, the properties of the surface-to-surface contact include:

- 202 • for the normal behaviour, a hard contact is assumed in all interaction surfaces to minimize  
203 any penetration of a slave surface to a master surface, and no transfer of tensile stress across  
204 the interface is allowed; and
- 205 • for the tangential behaviour, a penalty friction formulation with a friction coefficient of 0.5  
206 is used for all the surface-to-surface contact, except for the steel-deck contact pair which is  
207 assumed to be frictionless.

208

209 b) Quasi-static analysis with the dynamic/explicit method

210 In order to incorporate the complex contact conditions in the stud shear connections, and to  
211 model concrete crushing and cracking effectively, the quasi-static analysis with the  
212 dynamic/explicit method in the ABAQUS is adopted. Both numerical accuracy and  
213 computational efficiency of the finite element models are ensured with an introduction of a  
214 mass scaling as follows:

- 215 • The mass scaling factors of 1500, 1000, 500, 50 have been applied to the models, and the  
216 ratios of kinetic energy to internal energy (ALLKE/ALLIE) are monitored. A mass scaling  
217 of 500 is found to be appropriate while the value of ALLKE/ALLIE is found to be less than  
218 1%.

219 • The loading is applied in the form of a displacement control, and the development of the  
220 loading rate is defined with a smooth step function. This function is intended to smoothly  
221 ramp up the rate of loading application from zero to a specified magnitude over a short  
222 specified period of time. The loading rate is then kept constant for the rest of the analyses.  
223 The purpose of this loading method is to keep the magnitude of the kinetic energy at a very  
224 low level. Various loading rates of 5, 0.5, 0.05, and 0.01 mm/sec have been applied to the  
225 models in a sensitivity study. Based on the results of the study, a loading rate of 0.05 mm/sec  
226 is adopted for all subsequent analyses.

227

#### 228 c) Finite element analyses and convergence study

229 Typical finite element models for these shear connections are illustrated in Figure 4. Three  
230 shear connections with different configurations, as shown in Figure 5, have been successfully  
231 calibrated with the test results, noting that the names of the models are similar to those of the  
232 push-out tests.

233

234 A convergence study was carried out on finite element meshes with the concrete and the headed  
235 shear studs of different element sizes [22]. It should be noted that the most critical regions are  
236 often the shank roots of the headed shear studs and their surrounding concrete, and hence, these  
237 regions are systematically refined with reduced mesh sizes locally. After a convergence study  
238 with various mesh sizes of 15.0, 7.5, and 4.0 mm for the concrete, and of 12.0, 6.0, and 3.0 mm  
239 for the headed shear studs as shown in Figure 6, the key results are presented in Table 2. It is  
240 shown that a mesh size of 7.5 mm for the concrete and a mesh size of 6.0 mm for the shear  
241 studs are shown to be both structural accurate and computationally efficient, and hence, these  
242 element sizes were adopted for subsequent numerical investigations. Figure 5 plots both the  
243 measured and the predicted load-slippage curves of Models SS, SCFr, and SCUr onto the same  
244 graph for easy comparison, and both measured material and geometrical properties were  
245 adopted in the models. It is shown that the predicted curves of the three models were found to  
246 be very close to those obtained from the push-out tests.



247

248 This excellent comparison provides confidence in the accuracy of the advanced finite element  
249 models for these shear connections. Hence, the models can be used to predict with a high level  
250 of reliability the deformation characteristics of various types of stud shear connections,  
251 including capturing concrete crushing and cracking as well as shear yielding of headed shear  
252 studs. These numerical models are adopted in the present investigation for detailed assessments  
253 and parametric studies.

254

### 255 1.3 Shear resistances of shear connections in solid and composite slabs

256 Design methods for the shear resistances of stud shear connections with solid concrete slabs in  
257 several current codes of practice are based on the research work of Ollgaard et al. [33]. For  
258 example, in Cl. 6.6.3.1 of EN 1994-1-1 [23], the design shear resistance of a shear connection  
259 with headed shear studs fully embedded inside a solid concrete slab,  $Q_{SS}$ , is given by the  
260 smaller of the two values obtained from the following equations:

$$261 \quad Q_{m,CF} = 0.29d^2 \sqrt{f_{ck} E_{cm}} \times \frac{1}{\gamma_V} \quad (1a)$$

262 or

$$263 \quad Q_{m,SF} = 0.8f_u \left( \frac{\pi d^2}{4} \right) \times \frac{1}{\gamma_V} \quad (1b)$$

264 where  $f_{ck}$  is the characteristic cylinder compressive strength of the concrete;  $E_{cm}$  is the mean  
265 elastic modulus of the concrete;  $d$  is the diameter of the stud shank;  $f_u$  is the tensile strength of  
266 the stud shank, and  $\gamma_V$  is the partial factor with a recommended value of 1.25.

267

268 It should be noted that Equation (1a) relates to failure of the concrete while Equation (1b)  
269 relates to a shear failure of the steel stud [4]. According to Cl. 6.6.4.2 of EN 1994-1-1 [23],  
270 an additional shape factor,  $k_t$ , is introduced to the design shear resistance of the shear  
271 connection,  $Q_{SS}$ , to allow for the presence of the profiled decks which are perpendicular to  
272 supporting steel beams as follows:

273 
$$k_t = \frac{0.7 b_o}{\sqrt{n_r} h_p} \left( \frac{h}{h_p} - 1 \right) \quad (2)$$

274

275 where  $n_r$  is the number of shear stud(s) per trough;  $h$  and  $d$  are the height and the diameter of  
276 the shear stud, respectively; and  $h_p$  and  $b_o$  are the depth and the average width of the deck  
277 trough, respectively. It should also be noted that  $b_o$  is the average trough width for trapezoidal  
278 profiled decks, and is the minimum trough width for re-entrant profiled decks.

279

280 As various forms of profiled decks typically have longitudinal stiffeners in their troughs to  
281 improve their moment resistances, there are two different positions for the shear studs to be  
282 installed in the deck troughs, namely: i) a favourable position, and ii) an unfavourable position,  
283 as shown in Figure 1. It should be noted that these two positions in the deck troughs are  
284 classified according to different support and loading conditions of the composite floors. Various  
285 studies [2, 3, 5-8] have shown that there are significant differences in the deformation  
286 characteristics of composite beams with shear studs installed at different positions of the deck  
287 troughs. Hence, there is a need to develop design rules to assess the effects of installation  
288 positions of these shear studs in composite beams with profiled decks.

289

## 290 **2. Objectives and Scope of Work**

291 In order to examine the structural behaviour of stud shear connections in composite floors with  
292 various stud arrangements and profiled deck configurations, the validated finite element  
293 models, reported in Section 1.2 above, are employed herein in a detailed numerical  
294 investigation. A number of finite element models for typical shear connections in those  
295 composite beams with profiled decks spanning perpendicular to supporting steel beams are  
296 constructed, and a detailed assessment is conducted in order to identify various load transfer  
297 mechanisms. Moreover, parametric studies are performed with various stud arrangements and  
298 profiled deck configurations to assess the deformation characteristics of these shear  
299 connections.

300

301 It should be noted that the structural behavior of such shear connections is complex, and  
302 depends on several inter-independent parameters. It cannot, therefore, be adequately and  
303 practically quantified within an experimental assessment. To ensure that the numerical  
304 assessment provides information that enables focused quantification of the influence of key  
305 parameters, the following two main tasks were identified:

306

307 i) Task A Load transfer mechanism

308 A total of four finite element models of the stud shear connections with profiled decks  
309 were constructed, and non-linear analyses were performed in order to examine the “stress  
310 and strain” conditions of these connections at large deformations, based on which specific  
311 load transfer mechanisms within the shear connections can be identified and assessed; and

312

313 ii) Task B Parametric studies

314 A total of 16 finite element models of the stud shear connections were constructed and  
315 used to for parameter variations including the concrete cube strength, stud arrangements  
316 and profiled deck configurations, with a particular focus on their influence on the  
317 connection resistances.

318 It should be noted that in these parametric studies, a profiled deck of 1.0 mm thick and a  
319 yield strength of  $280 \text{ N/mm}^2$  was used; headed shear studs of a shank diameter of 19 mm  
320 and a welded height at 95 mm were adopted; the tensile strength of the shear studs after  
321 cold forging was assumed as  $450 \text{ N/mm}^2$ ; the height and the diameter of welding collars  
322 of headed shear studs were assumed to be 3 and 25 mm respectively; and pairs of headed  
323 shear studs were installed at a transverse spacing of 100 mm.

324

325 The key areas of interest of the numerical investigations include:

326 i) internal force distributions within various shear connections, and their corresponding load  
327 transfer mechanisms;

- 328 ii) typical failure modes of the shear connections with various stud arrangements and profiled  
329 deck configurations; and  
330 iii) effects of longitudinal stiffeners in the deck troughs on the deformation characteristics of  
331 the shear connections.

332

333 Based on the results of the detailed numerical investigations, a configuration parameter,  $\beta$ , is  
334 proposed to allow for any reduction in the shear resistance of the connections due to the effects  
335 of various stud arrangements and profiled deck configurations.

336

337 It should be noted that after successful completion of these numerical investigations, it is  
338 possible to examine structural behaviour of shear connections with different combinations of  
339 stud arrangements in the deck troughs, for example, staggered or alternate arrangements of  
340 studs in either “favourable” or “unfavourable” positions.

341

### 342 **3. Load Transfer Mechanisms**

343 The position of the shear studs in the deck troughs (i.e. favourable or unfavourable) has a direct  
344 effect on the connection behaviour in the push-out tests. In order to quantify the structural  
345 behaviour of these stud shear connections with various stud arrangements and profiled deck  
346 configurations, the following four models are established:

347

- 348 • Model SS is established to model typical shear connections with solid concrete slabs, and  
349 it is a reference model for comparison with the other three models with profiled decks.  
350
- 351 • Model SC represents typical shear connections in composite beams with profiled deck in  
352 which the shear studs are installed at the centers of the deck troughs.  
353
- 354 • Models SCFr and SCUr are variants of Model SC, in which the shear studs are installed at  
355 the favourable and the unfavourable positions in the deck troughs, respectively.

356

357 It should be noted that Models SS, SCFr and SCUr have been directly calibrated against test  
358 results as described in Section 1.2. However, no calibration for Model SC against test data is

359 possible owing to the presence of longitudinal stiffeners at the centers of the deck troughs, and  
360 hence, headed shear studs cannot be physically installed at the centers of the deck troughs.

361

### 362 3.1 Numerical results

363 The four models provided detailed results which were used to examine the failure conditions.  
364 For each model, the following results are extracted: i) a two-dimensional deformed mesh  
365 showing deformations of the shear studs, and highly localized areas in terms of concrete  
366 stresses, and ii) a simplified force diagram of the connection. It should be noted that  $F_v$ ,  $F_c$  and  
367  $M$  are the internal shear force, the internal tension force and the local moment at the root of the  
368 headed shear stud, respectively; while  $F_{\text{fict}}$  is the total frictional force of the shear connection  
369 between the concrete and the top surface of the steel flange or the profiled deck. The numerical  
370 results for all four models are presented collectively together in Figure 7 for direct comparison.  
371 Moreover, in order to present clear illustrations of damaged concrete in these models, three-  
372 dimensional images of concrete crushing and cracking are also provided, related to which the  
373 following definitions of concrete failure are adopted:

- 374 i) a concrete crushing zone is identified in term of a compressive equivalent plastic strain,  
375 PEEQ [26], and it is assumed that those concrete elements with a PEEQ value exceeding  
376 0.005 have crushed [21, 22]; and  
377 ii) a concrete cracking damage is considered in term of a cracking displacement using a  
378 function of DAMAGET [26], and it is assumed that concrete elements with a DAMAGET  
379 reaching a value of 1.0 have cracked.

380

381 Both the cracking and the crushing zones of the damaged concrete in the four models are  
382 highlighted in different colors in Figure 7. It is shown that:

383

- 384 a) In Model SS, the applied loads are transferred from the steel section to the concrete slabs  
385 through the shear studs, i.e. through *shear action*, which are in turn transferred onto the  
386 surrounding concrete through *local bearing*. These *bearing forces* are readily built up at  
387 the roots of the studs where many concrete elements are highly stressed under

388 compression; the bearing forces diminish quickly as they move away from the steel-  
389 concrete interface. As there are many concrete elements available in the concrete slab  
390 to receive the *applied forces*, a conical concrete failure over a large area of concrete is  
391 unlikely to take place. Instead, the connection typically fails in stud shear failure at a large  
392 deformation beyond 6 mm.

393

394 b) In Model SC, the applied loads are transferred from the steel section to the composite  
395 slab, i.e. the continuous portion of the concrete slab, through the shear studs. These *shear*  
396 *forces* are in turn transferred onto the surrounding concrete through *local bearing* acting  
397 on the shear studs. The *bearing forces* are readily built up at the roots of the studs though  
398 they diminish quickly once they move away from the steel-concrete interface. Owing to  
399 the presence of the profiled deck, or more precisely, an absence of the corresponding  
400 concrete elements, there are only limited concrete elements behind the shear studs, and  
401 hence, the load transfer from these ‘trough’ concrete onto the ‘slab’ concrete may become  
402 critical. Hence, a conical concrete failure over the ‘slab’ concrete in the shear connection  
403 is often critical, and the corresponding shear resistance of the shear connection is  
404 significantly reduced, when compared with that of Model SS. Moreover, as all these  
405 forces act eccentrically to the ‘slab’ concrete, local moments are induced, and many  
406 elements in the continuous portion of the slab are cracked.

407

408 c) Similar to the load path established in Model SC, the applied loads in both Models SCFr  
409 and SCUr are shown to be readily transferred from the steel sections to the continuous  
410 portions of the composite slabs through the shear studs. These *shear forces* are transferred  
411 from the shear studs onto the surrounding concrete through *local bearing*. However,  
412 depending on the amount of the ‘trough’ concrete receiving these bearing forces, there  
413 are two different mechanisms:

414 • In Model SCFr, owing to the presence of a relatively large lump of ‘stiff and strong’  
415 concrete in the ‘trough’ behind the shear studs, it receives the bearing forces readily  
416 as compressive forces, and transfers them into shear forces acting onto the continuous  
417 portion of the composite slab without causing any significant deformation in the stud.

418 At the same time, this lump of “trough” concrete is subjected to

419 i) the bearing forces acting close to the shank roots of the studs, and

420 ii) the reaction forces acting along the continuous portion of the concrete slab.

421

422 Hence, this lump of “trough” concrete together with neighbouring “slab” concrete is  
423 under a large local moment, and they tend to rotate as a whole. As the applied shear  
424 forces increase in magnitude, a conical failure will take place in the “slab” concrete  
425 under the action of the tension forces induced by the moments. It should be noted that  
426 this is a non-ductile mode of failure.

427

- 428 • In Model SCUr, there is only a small lump of “trough” concrete behind the shear studs  
429 which is not stiff nor strong enough to receive the applied forces, and hence, this  
430 “trough” concrete is unable to provide an effective load path, i.e. from bearing forces  
431 to compressive forces, to transfer the applied forces to the continuous portion of the  
432 composite slab. Instead, the studs receive the applied forces directly at their shank  
433 roots while their shanks deform readily into a double curvature under shear action,  
434 i.e. a dowel mechanism, to transfer the applied forces while most of the neighbouring  
435 “trough” concrete is cracked. In general, this is a highly ductile mode because of the  
436 dowel mechanism of the shear studs.

437

438 For ease of presentation, ductility of the stud shear connections is classified as follows:

- 439 • highly ductile when  $s_u \geq 5.5$  mm, and  $s_u - s_m = 3.5 \sim 4.5$  mm
- 440 • ductile when  $s_u = 4.5 \sim 5.5$  mm; and  $s_u - s_m = 2.5 \sim 3.5$  mm
- 441 • non-ductile when  $s_u \leq 4.5$  mm, and  $s_u - s_m = 1.0 \sim 2.5$  mm

442 where

443  $s_m$  is the slippage corresponding to  $Q_m$ ; and

444  $s_u$  is the slippage corresponding to  $0.8 Q_m$  (unloading).

445

### 446 3.2 Load paths within connections

447 In order to provide an overall understanding of various load transfer mechanisms within the  
448 shear connections, simplified load paths of all the four models are illustrated in Figure 8. In  
449 general, the structural behaviour of Model SS (i.e. the stud shear connections with solid  
450 concrete slabs) depends primarily on the highly compressed concrete behind the shear studs.  
451 As these concrete areas are relatively stiff and strong, only local concrete crushing takes place,  
452 and the critical failure mode of the connection is shear-off failure of the steel stud.

453

454 For those shear connections with various stud arrangements and profiled deck configurations,  
455 various parts and extents of the concrete are cracked and crushed, as shown in Figure 8,  
456 depending on their different positions in the deck troughs. They may be broadly classified as:

457

458 i) Large concrete behind shear studs with a non-ductile failure

459 In Model SCFr, large “trough” concrete are ‘stiff and strong’, and they are able to stand the  
460 bearing forces from the shear studs. These forces are readily received by the ‘trough’  
461 concrete as compression forces, and then transferred onto the ‘slab’ concrete through shear  
462 action. Essentially, the load path goes through the “trough” concrete, and a non-ductile  
463 conical shear failure of the concrete is often critical.

464

465 ii) Sufficient concrete behind shear studs with a ductile failure

466 In Model SC, the “trough” concrete is sufficiently effective to transfer compression forces,  
467 when compared with that in Model SCFr. Moreover, the dowel mechanism is effective to  
468 maintain the shear resistances under a limited slippage. Essentially, the load path goes  
469 through the “trough” concrete, and a conical failure in the concrete often becomes critical  
470 at large deformations.

471

472 iii) Small concrete behind shear studs with a highly ductile failure

473 In Model SCUr, the ‘trough’ concrete is unable to transfer compression forces effectively.  
474 Instead, the applied forces are transferred through a dowel mechanism of the shear studs,  
475 i.e. the stud shanks are bent into a double curvature so that the applied forces are transferred  
476 into the ‘slab’ concrete through the embedded heads of the shear studs. Essentially, the load  
477 path goes through the shear studs, which fail under combined shear and bending in a highly  
478 ductile manner.

479

480 For detailed discussions on both the forces and the moments along the lengths of the headed  
481 shear studs within these connections, refer to References 21 and 22.

482

#### 483 **4. Parametric Assessments**

484 In order to generate design data for assessing the shear resistance of the stud shear connections  
485 with various stud arrangements and profiled deck configurations, detailed parametric studies



486 were undertaken using the validated finite element models presented above. Key parameters  
487 considered include:

- 488 • Installation positions of shear studs

489 For each connection, the shear studs are installed at one of the three positions of the deck  
490 troughs, namely:

- 491 i) central position, denoted as “C”,
- 492 ii) favourable position, denoted as “F”, and
- 493 iii) unfavourable position, denoted as “U”.

- 494 • Configuration of profiled decks

495 For each connection, the trough widths of the deck,  $b_o$ , are assigned as 110, 135 or 160  
496 mm, while the deck height is assumed to be 50 mm in all cases. In the presence of  
497 longitudinal stiffeners in the central positions of the deck troughs, their height is  
498 considered as 10 mm in all cases, and this is denoted as “r”.

499

500 Figure 9 depicts a total of 16 finite element models established for the present parametric  
501 studies, and Table 3 summarizes the programme of the parametric studies together with key  
502 results. It should be noted that all the numerical results provided above are based on a tensile  
503 strength of  $450 \text{ N/mm}^2$  for the stud steel, and a cube strength of  $30 \text{ N/mm}^2$  for the concrete  
504 material. Comparative assessments of the numerical results are presented below.

505

#### 506 4.1 Study PS01

507 In this study, the shear resistances of the stud shear connections with installation positions at  
508 C, F and U, and trough width  $b_o = 160, 135, \text{ and } 110 \text{ mm}$ , are compared as follows:

- 509 a) Model SS results in high strength and ductility; a shear resistance of 105.1 kN per stud is  
510 attained, i.e.  $Q_{SS} = 105.1 \text{ kN}$ . The load-slippage curve is depicted in various graphs, as  
511 shown in Figure 10, and considered as the reference curve for comparison.
- 512 b) All the deformation characteristics of various groups of these shear connections are  
513 plotted in the same graphs in Figure 10 for direct comparison. It is shown that all load-

514 slippage curves of Models SC-C (with various trough widths) may be regarded as ductile,  
515 while those of Models SC-F and SC-U are considered to be non-ductile and highly ductile  
516 respectively.

517 c) In the presence of the profiled deck with trough widths of 160, 135 and 110 mm,  
518 significant reduction in the shear resistances of the connections occurs. In general, the  
519 reduction factors for Models SC-160F, -135F and -110F are found to be 0.80, 0.75 and  
520 0.65, respectively. For Models SC-160C, SC-135C and SC-110C, the corresponding  
521 reduction factors are found to be 0.73, 0.69 and 0.62 respectively. For Models SC160-U,  
522 SC-135U and SC-110U, the corresponding reduction factors are found to be 0.75, 0.68  
523 and 0.62 respectively.

524 d) Accordingly, when the shear studs are installed at the favourable positions in the deck  
525 troughs, instead of the central positions, the corresponding reduction factors are increased  
526 by values of 0.06 to 0.07 when  $b_o = 160$  or 135 mm.

527

## 528 4.2 Study PS02

529 In this study, the shear resistances of the stud shear connections with installation positions at  
530 C, F & Fr, and U & Ur, and trough width  $b_o = 160, 135,$  and 110 mm are compared. The  
531 deformation characteristics of various model groups are plotted in the same graphs for direct  
532 comparison in Figures 11, 12 and 13, and these deformation characteristics are shown to be  
533 very similar among those stud shear connections with the same installation positions, as  
534 discussed in the section above. It is shown that:

535

536 a) Model SS results in high strength and ductility; a shear resistance of 105.1 kN per stud is  
537 attained, i.e.  $Q_{SS} = 105.1$  kN. The load-slippage curve is used as the reference curve.  
538 Similarly, the load-slippage curves of Models SC-110C, SC-135C, and SC-160C are also  
539 adopted as basic curves for subsequent comparisons with shear connections with various  
540 stud arrangements and profiled deck configurations. It should be noted that their shear  
541 resistances are found to be 0.62, 0.69, and 0.73  $Q_{SS}$  respectively.

542

543 b) When the headed shear studs are installed at the favourable positions in the deck troughs,  
544 i.e. Models SC-160F, SC-135F, and SC-110F, the shear resistances of the shear  
545 connections are 0.80, 0.75, and 0.65  $Q_{ss}$ . However, in the presence of longitudinal  
546 stiffeners in the deck troughs, i.e. Models SC-160Fr, SC-135Fr, and SC-110Fr, the shear  
547 resistances of the shear connections are further reduced to 0.74, 0.68, and 0.58  $Q_{ss}$   
548 respectively. Both load-slippage curves are considered non-ductile.

549

550 c) When the headed shear studs are installed in the unfavourable positions in the troughs of  
551 the deck, i.e. Models SC-160U, SC-135U, and SC-110U, the shear resistances of the shear  
552 connections are found to be 0.75, 0.68, and 0.62  $Q_{ss}$ . In the presence of longitudinal  
553 stiffeners in the troughs of the deck, i.e. Models SC-160Ur, SC-135Ur, and SC-110Ur,  
554 the shear resistances of the connections are further reduced to 0.58, 0.50, and 0.42  $Q_{ss}$ .  
555 However, the load-slippage curves are highly ductile.

556

557 The equivalent compressive plastic strains, PEEQ, in the concrete slabs of various models are  
558 also illustrated in Figures 11, 12, and 13 for direct comparison. In general, their patterns in  
559 the stud shear connections with various connector arrangements and profiled deck  
560 configurations are shown to be very similar.

561

#### 562 4.3 Shear resistances of stud shear connections

563 In order to provide data on the shear resistances of these stud shear connections with various  
564 concrete grades, an extensive set of 80 analyses was carried out with concrete compressive  
565 strengths ranging from 30 N/mm<sup>2</sup> to 50 N/mm<sup>2</sup>. The predicted shear resistances per stud for  
566 connections with various groups of stud arrangements and profiled deck configurations are  
567 plotted in the same graphs for direct comparison, as shown in Figures 14, 15 and 16. It is shown  
568 in the figures that:

569 • By increasing the concrete cube strengths  $f_{cu}$  from 30 to 50 N/mm<sup>2</sup>, the shear resistance

570 of the stud shear connections, for various arrangements, increases slightly.

571 • The installation positions of the studs in the profiled deck are very important, and the  
572 presence of a sufficiently large concrete area behind the shear studs increases the shear  
573 resistances of the shear connections.

574 • By reducing the trough widths  $b_o$  from 160 to 110 mm, the shear resistance of the  
575 connections decreases slightly.

576 • The presence of longitudinal stiffeners in the deck troughs reduces the shear resistances  
577 of the connections significantly when the shear studs are installed in the unfavourable  
578 positions in the deck troughs.

579

580 In order to capture the influence of stud arrangements and profiled deck configurations, a  
581 configuration parameter  $\beta$  is proposed in conjunction with the reduction factor  $k_t$ . The  
582 suggested design approach is therefore given as follows:

583

$$584 \quad Q_m = \beta \times k_t \times \min\{ Q_{m,CF}, Q_{m,SF} \} \quad (3)$$

585

586 where:  $Q_{m,CF}$  and  $Q_{m,CF}$  are given by Equations (1a) and (1b) with the partial factor  $\gamma_v$  equal to  
587 1.0,  $k_t$  is the reduction factor given by Equation (2); and  $\beta$  is a configuration factor proposed in  
588 this study based on the results of the parametric studies, with the values of  $\beta$  as given in Table 4.

589

590 In general, the values of  $\beta$  depend on the geometry as well as the dimensions of the profiled  
591 deck, including the heights and widths of the troughs, and the heights of the longitudinal  
592 stiffeners, if any. It should be noted that:

593 i) for shear connections with profiled deck with  $b_o$  at 160 mm, the values of  $\beta$  range from  
594 1.00 to 0.75.

595 ii) for shear connections with profiled deck with  $b_o$  at 135 mm, the values of  $\beta$  range from  
596 0.95 to 0.65; and

597 iii) for shear connections with profiled deck with  $b_o$  at 110 mm, the values of  $\beta$  range from  
598 0.85 to 0.55.

599

## 600 **5. Conclusions**

601 This paper presents a detailed study into the structural behaviour of stud shear connections with  
602 various commonly used stud arrangements and profiled deck configurations. In order to  
603 examine and quantify the behaviour, a detailed numerical investigation is carried out followed  
604 by a parametric assessment covering a wide range of practical shear connections with both  
605 solid concrete slabs and composite slabs. The main findings of the study can be summarized as  
606 follows:

607

608 a) Based on the numerical results of the experimentally validated and calibrated finite  
609 element models, the detailed stress distributions of various stud shear connections were  
610 used in order to identify the underlying load transfer mechanisms. Simplified load paths  
611 within these models were also highlighted by considering the ‘stress and strain’ plots of  
612 the models at failure, and three dimensional plots of the damaged concrete. It was shown  
613 that the effectiveness of the ‘trough’ concrete in resisting the applied loads, and then  
614 transferring them to the ‘slab’ concrete is vital in determining the structural behaviour of  
615 these stud shear connections. When there are sufficiently large concrete areas behind the  
616 shear studs, the connection exhibits a relatively high shear resistance, but a non-ductile  
617 load-slippage curve. In contrast, when there is only limited concrete behind the shear  
618 studs, the connection has a relatively low shear resistance but a highly ductile load-  
619 slippage curve as it is the shear studs that determine the ultimate behaviour.

620 b) The results of parametric studies on the shear connections, with various stud  
621 arrangements and profiled deck configurations, enable a comparison of the load-slippage  
622 curves and shear resistances against those of shear connections with solid concrete slabs.  
623 It is shown that shear connections with solid concrete slabs consistently offer high  
624 strength and ductility. However, in the presence of profiled decks, the load-slippage  
625 curves of those connections with shear studs installed at the favourable or the  
626 unfavourable positions are very different. The load-slippage behaviour of Model SS is  
627 considered to be highly ductile while that of Model SC is considered to be ductile. On the

628 other hand, Models SC-F and SC-U result in a non-ductile and a highly ductile response,  
629 respectively.

630

631 c) In order to assess the effects of stud arrangements and profiled deck configurations on  
632 the shear resistances of the shear connections, a total of 80 finite element analyses were  
633 performed. A configuration parameter  $\beta$  is proposed, based on the results of these  
634 analyses, to be used in conjunction with the reduction factor  $k_t$  adopted in EN 1994-1-1.  
635 It should be noted that the values of  $\beta$  are found numerically to range from 0.55 to 1.0 for  
636 various installation positions of headed shear studs, trough widths of the profiled decks,  
637 and the presence of longitudinal stiffeners, if any.

638

639 Overall, this paper provides detailed insights into the structural behaviour of the stud shear  
640 connections including the load transfer mechanisms. This investigation also quantifies the  
641 reduction in the shear resistances of these shear connections with various stud arrangements  
642 and profiled deck configurations. The effects of these reductions are considerably more  
643 pronounced than those commonly allowed for in the design of stud shear connections in  
644 composite structures, and point to the need for modification of current codified procedures.

645

646

647

#### 648 **Acknowledgements**

649 The research project leading to publication of this paper is funded by the Research Grants  
650 Council of the University Grants Committee of the Government of Hong Kong SAR (Project  
651 No. PolyU 5143/13E), and the Chinese National Engineering Research Centre for Steel  
652 Construction (Hong Kong Branch) funded by the Innovation and Technology Commission of  
653 the Government of Hong Kong SAR, and the Research Committee of the Hong Kong  
654 Polytechnic University. The research work reported in this paper is part of the research study  
655 of the first author at The Hong Kong Polytechnic University. Moreover, the supply and  
656 fabrication of the steel sections of the test specimens by Wo Lee Steel Co. Ltd., Genyield  
657 Construction Co. Ltd., and STAM Steel Co. Ltd. are gratefully acknowledged.

658

659 **References**

660

661 [1] D.J. Oehlers, R.P. Johnson. The strength of stud shear connections in composite beams. *The Structural*  
662 *Engineer*. 65 (1987), 44-48.

663 [2] J.T. Mottram, R.P. Johnson. Push tests on studs welded through profiled steel sheeting. University of  
664 Warwick 1989.

665 [3] R.P. Johnson, H. Yuan. Existing rules and new tests for stud shear connectors in troughs of profiled sheeting.  
666 *P I CIVIL ENG-STR B*. 128 (1998), 244-251.

667 [4] D. Lam, E. El-Lobody. Behavior of headed stud shear connectors in composite beam. *J STRUCT ENG*. 131  
668 (2005), 96-107.

669 [5] J. Qureshi, D. Lam, J. Ye. Effect of shear connector spacing and layout on the shear connector capacity in  
670 composite beams. *J CONSTR STEEL RES*. 67 (2011), 706-719.

671 [6] J. Qureshi, D. Lam, J. Ye. The influence of profiled sheeting thickness and shear connector' s position on  
672 strength and ductility of headed shear connector. *ENG STRUCT*. 33 (2011), 1643-1656.

673 [7] E. Ellobody, B. Young. Performance of shear connection in composite beams with profiled steel sheeting. *J*  
674 *CONSTR STEEL RES*. 62 (2006), 682-694.

675 [8] J. Qureshi, D. Lam. Behaviour of headed shear stud in composite beams with profiled metal decking. *ADV*  
676 *STRUCT ENG*. 15 (2012), 1547-1558.

677 [9] F. Tahmasebinia, G. Ranzi, A. Zona. Probabilistic three-dimensional finite element study on composite  
678 beams with steel trapezoidal decking. *J CONSTR STEEL RES*. 80 (2013), 394-411.

679 [10] U. Katwal, Z. Tao, M.K. Hassan. Finite element modelling of steel-concrete composite beams with profiled  
680 steel sheeting. *J CONSTR STEEL RES*. 146 (2018), 1-15.

681 [11] V. Vigneri, C. Odenbreit, M. Braun. Numerical evaluation of the plastic hinges developed in headed stud  
682 shear connectors in composite beams with profiled steel sheeting. *Structures* (2019).

683 [12] D.J. Oehlers, M.A. Bradford. *Composite steel and concrete structural members: fundamental behaviour*.  
684 Oxford: Pergamon Press 1995.

685 [13] R.P. Johnson, R.J. Buckby. *Composite Structures of Steel and Concrete*. Wiley Online Library 1975.

686 [14] S. Hicks. Strength and ductility of headed stud connectors welded in modern profiled sheeting. *Structural*  
687 *Engineer*. 85 (2007), 32-39.

688 [15] G. Ranzi, M.A. Bradford, P. Ansourian, A. Filonov, K. Rasmussen, T.J. Hogan, B. Uy. Full-scale tests on  
689 composite steel - concrete beams with steel trapezoidal decking. *J CONSTR STEEL RES*. 65 (2009), 1490-  
690 1506.

691 [16] O. Mirza, B. Uy. Effects of the combination of axial and shear loading on the behaviour of headed stud steel  
692 anchors. *ENG STRUCT*. 32 (2010), 93-105.

693 [17] Z. Lin, Y. Liu, J. He. Behavior of stud connectors under combined shear and tension loads. *ENG STRUCT*.  
694 81 (2014), 362-376.

695 [18] M.H. Shen, K.F. Chung. Experimental investigation into stud shear connections under combined shear and  
696 tension forces. *J CONSTR STEEL RES*. 133 (2017), 434-447.

697 [19] Q. Sun, X. Nie, M.D. Denavit, J. Fan, W. Liu. Monotonic and cyclic behavior of headed steel stud anchors  
698 welded through profiled steel deck. *J CONSTR STEEL RES*. 157 (2019), 121-131.

699 [20] B. Lu, C. Zhai, S. Li, W. Wen. Predicting ultimate shear capacities of shear connectors under monotonic and  
700 cyclic loadings. THIN WALL STRUCT. 141 (2019), 47-61.

701 [21] M.H. Shen, K.F. Chung. Structural behaviour of stud shear connections with solid and composite slabs under  
702 co-existing shear and tension forces. Structures. 9 (2017), 79-90.

703 [22] M.H. Shen. Structural behavior of shear connections in composite structures under complex loading  
704 conditions. PhD thesis. The Hong Kong Polytechnic University (2013).

705 [23] BSI. BS EN 1994-1-1: 2004. Eurocode 4: Design of Composite Steel and Concrete Structures. Part 1-1:  
706 General rules and rules for buildings. British Standards Institution (2004).

707 [24] BSI. BS 5950: Structural Use of Steelwork in Building. Part 3 Section 3.1: Code of Practice for Design of  
708 Composite Beams. British Standards Institution (1990).

709 [25] BSI. BS EN ISO 6892-1: Metallic materials – Tensile testing. Part 1: Method of test at ambient temperature.  
710 British Standards Institution (2009).

711 [26] Abaqus. Abaqus User's Manual, Version 6.14. Dassault Systemes Simulia Corp.2014.

712 [27] B. Alfarah, F. López-Almansa, S. Oller. New methodology for calculating damage variables evolution in  
713 Plastic Damage Model for RC structures. ENG STRUCT. 132 (2017), 70-86.

714 [28] J. Lubliner, J. Oliver, S. Oller, E. Oñate. A plastic-damage model for concrete. INT J SOLIDS STRUCT. 25  
715 (1989), 299-326.

716 [29] J. Lee, G.L. Fenves. Plastic-damage model for cyclic loading of concrete structures. J ENG MECH. 124  
717 (1998), 892-900.

718 [30] BSI. BS EN 1992-1-1: 2004. Eurocode 2: Design of Concrete Structures. Part 1-1: General rules and rules  
719 for buildings. British Standards Institution (2004).

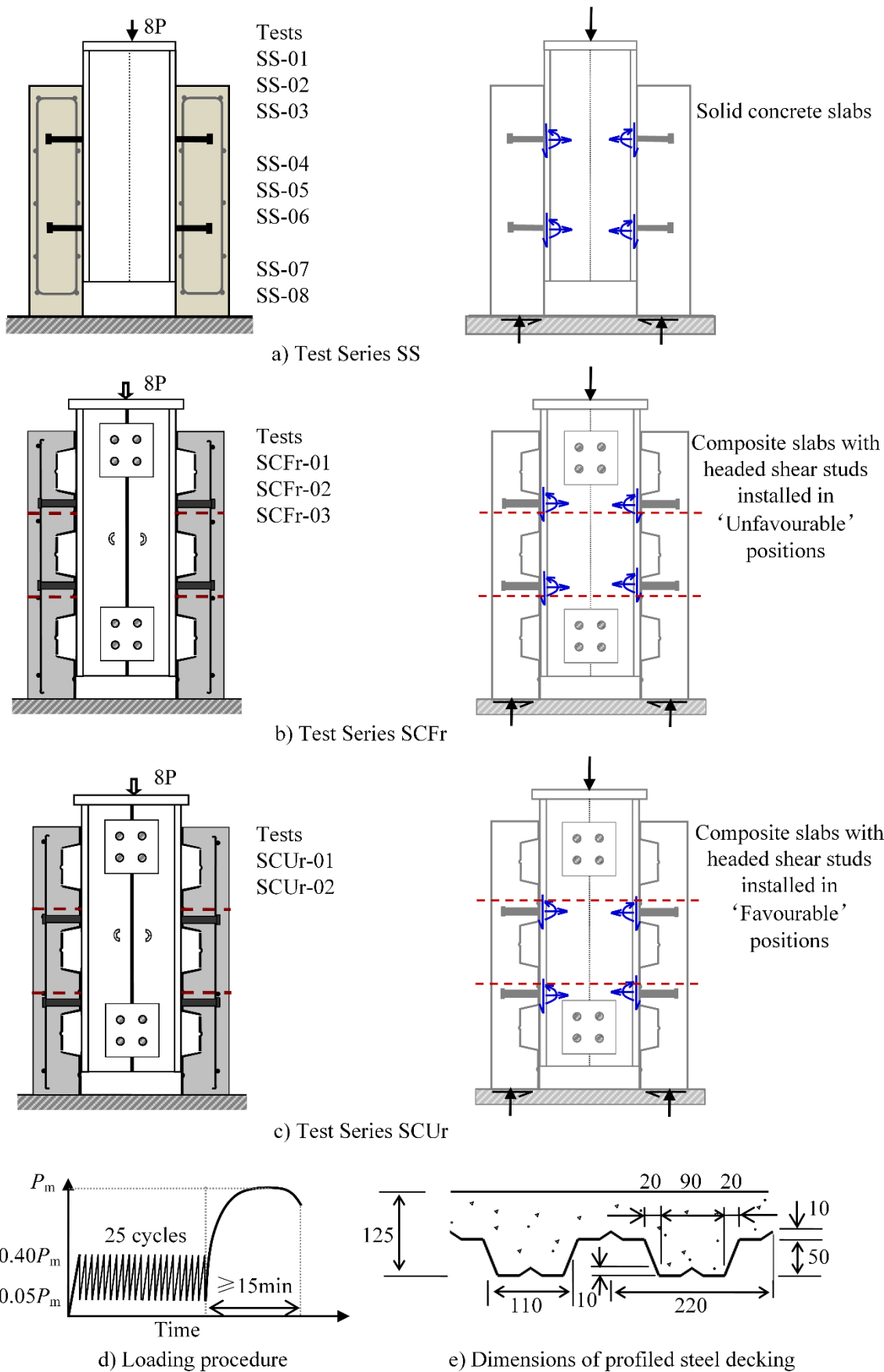
720 [31] BD. Code of Practice for the Structural Use of Concrete. Buildings Department of the Government of Hong  
721 Kong (2004).

722 [32] CEB. CEB-FIP Model Code. Comité Euro-International du Béton, Thomas Telford, London (2010).

723 [33] J.G. Ollgaard, R.G. Slutter, J.W. Fisher. Shear strength of stud connectors in lightweight and normal weight  
724 concrete. Engineering Journal-American Institute of Steel Construction (1971).

725





1  
2  
3  
4

Figure 1: Push-out tests conducted by Shen and Chung [18]

5



6

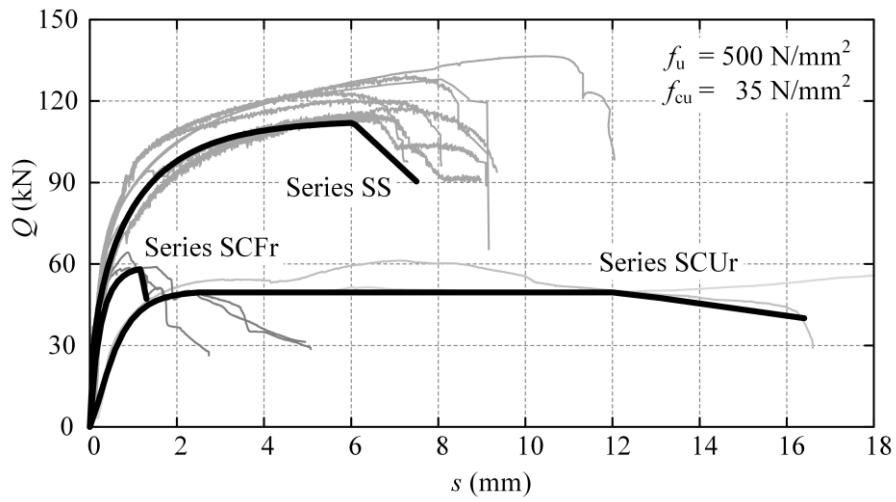
7

8

9

10

Figure 2: Typical concrete conical failure in shear connections with composite slabs



11

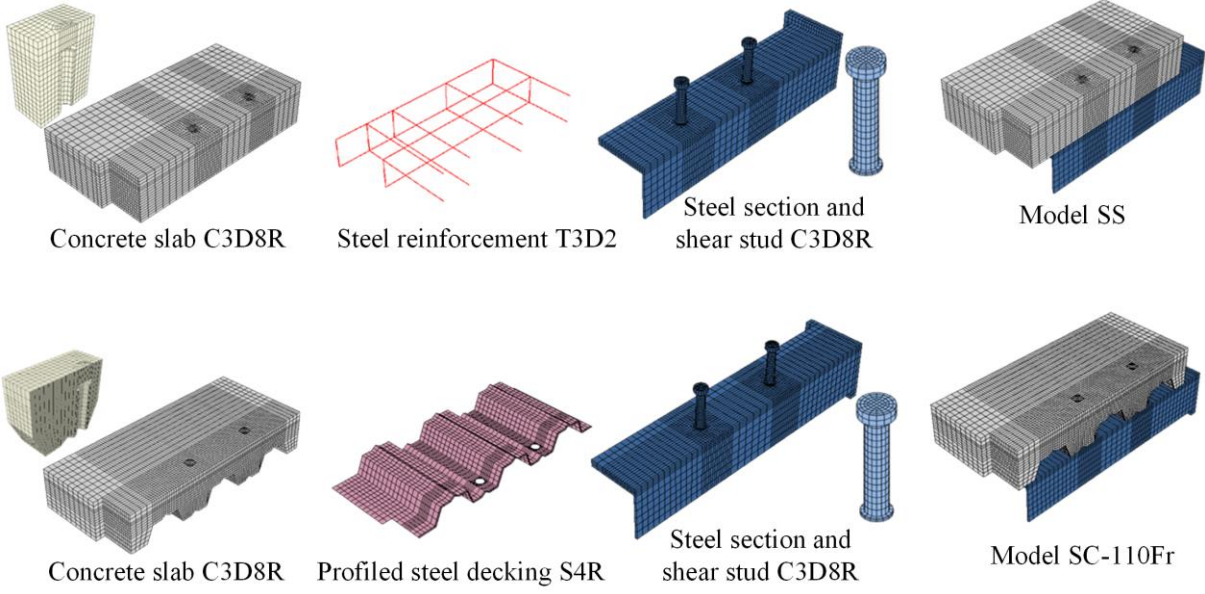
12

13

14

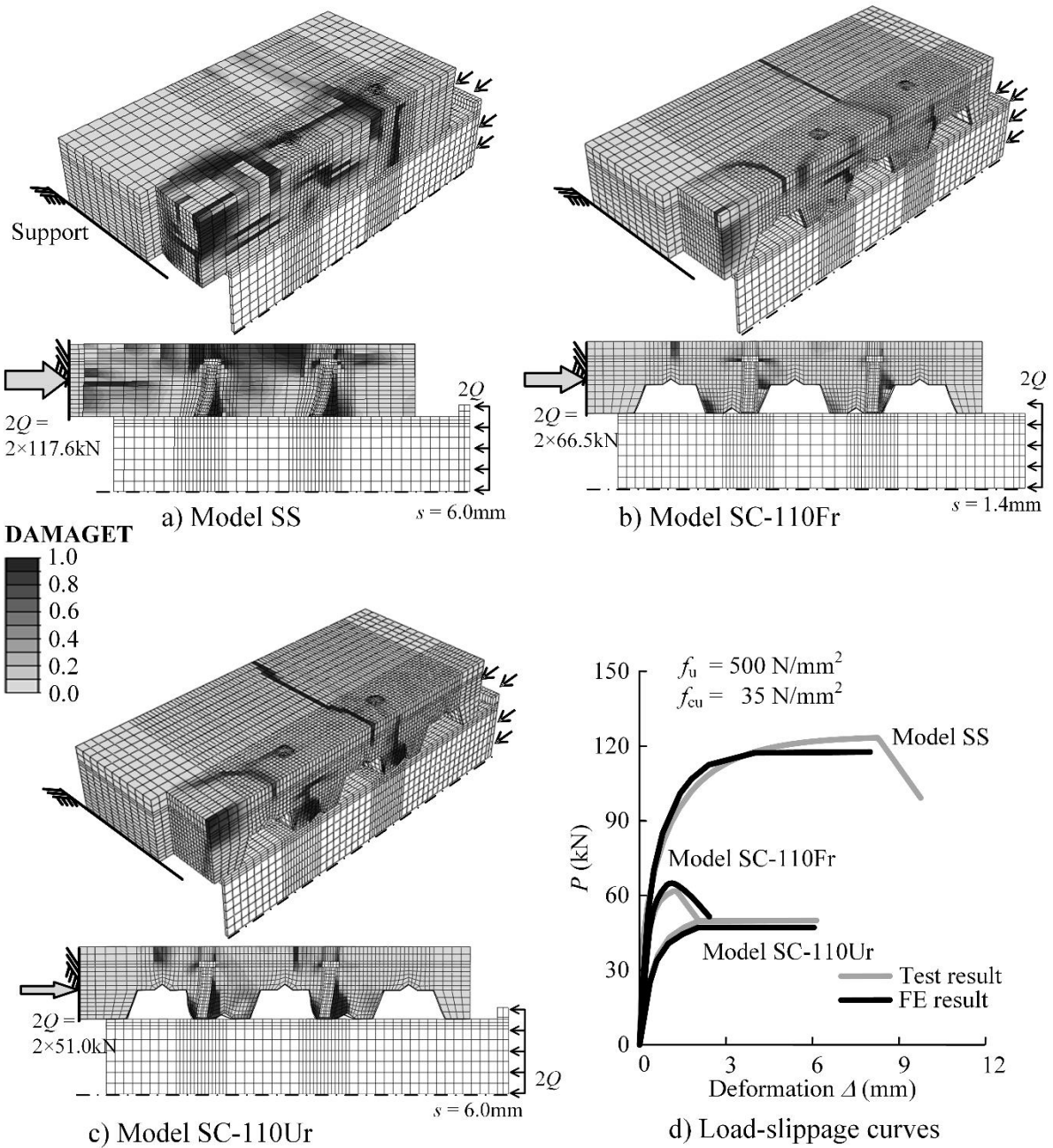
15

Figure 3: Standardized load-slippage curves of push-out tests



16  
17  
18

Figure 4: Finite element modelling

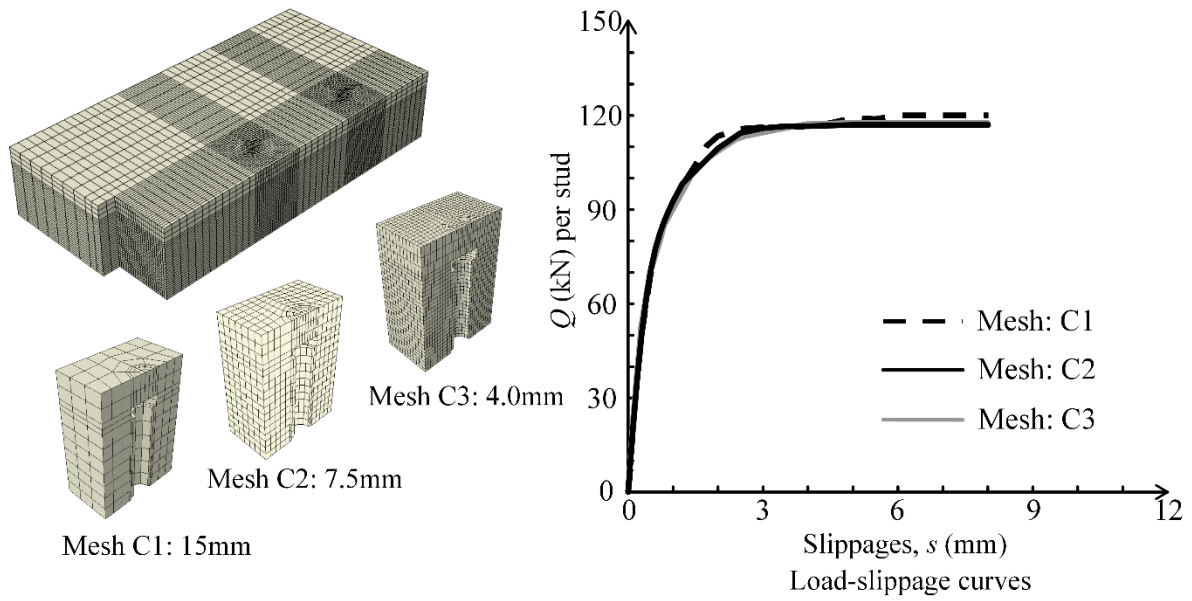


19

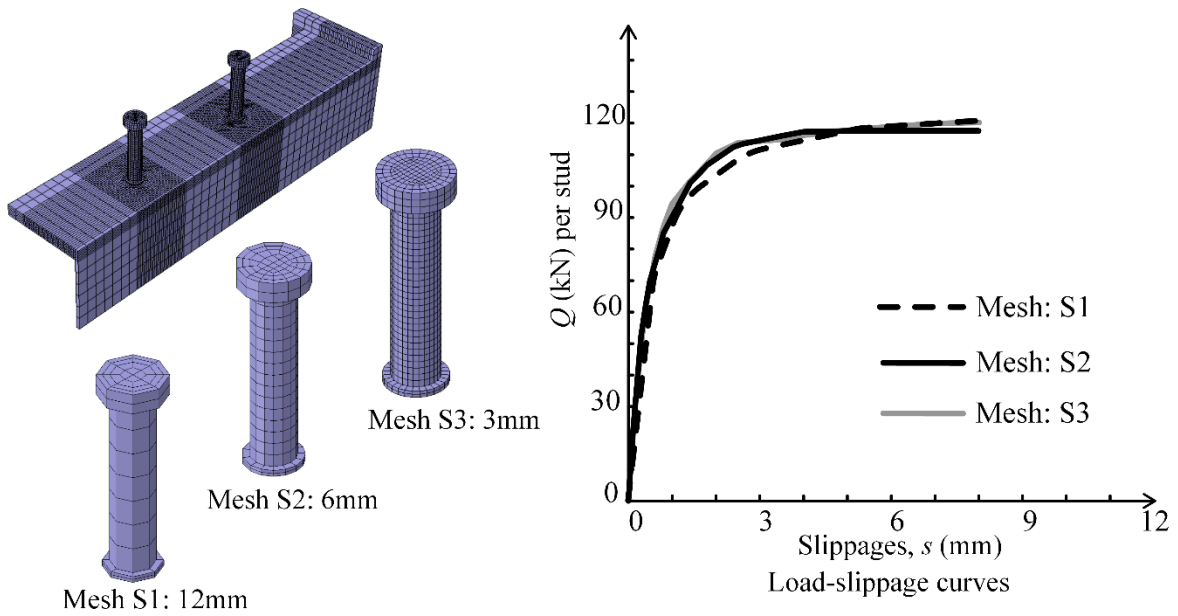
20

21

Figure 5: Numerical results of Models SS and SC



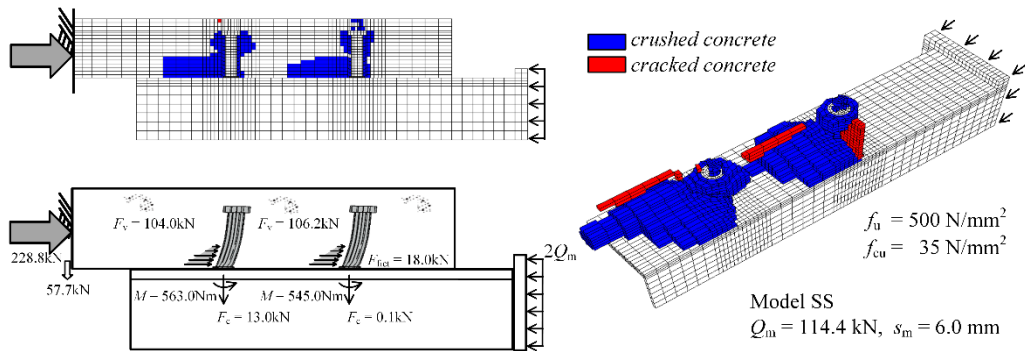
a) Various mesh sizes of the concrete slabs



b) Various mesh sizes of the headed shear studs

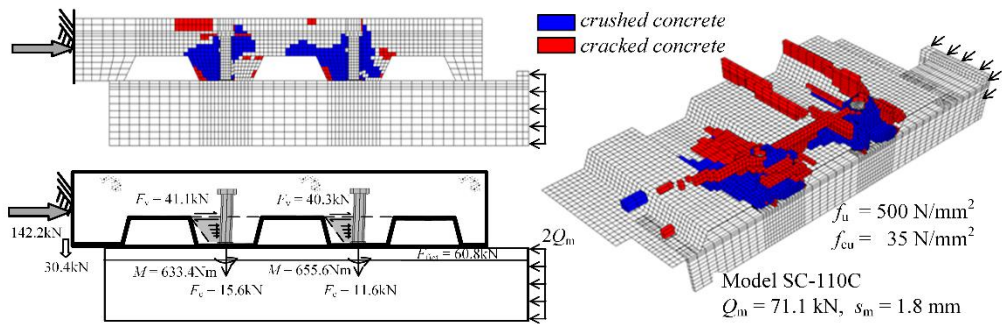
22  
23  
24  
25  
26  
27  
28  
29  
30  
31  
32

Figure 6: Predicted load-slippage curves of Models SS with different element sizes



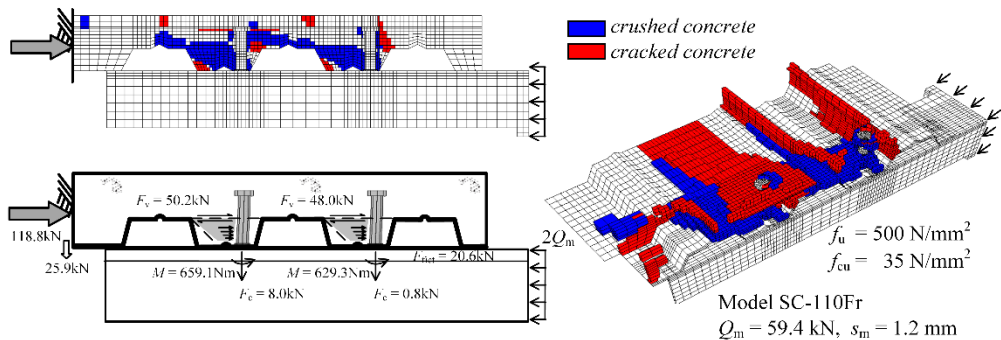
33  
34

a) Model SS



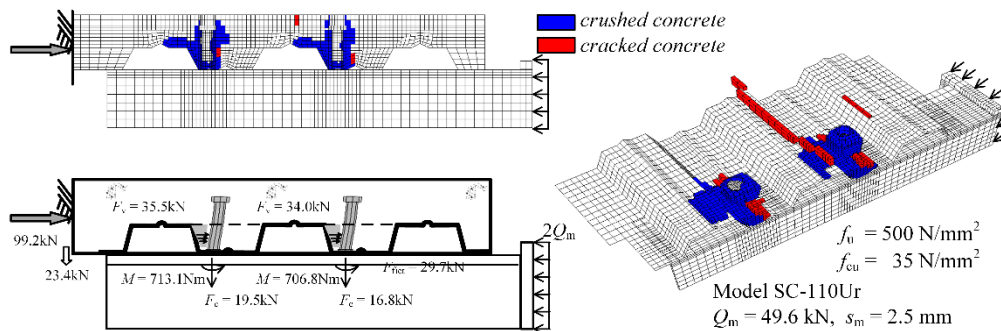
35  
36

b) Model SC-110C



37  
38

c) Model SC-110Fr



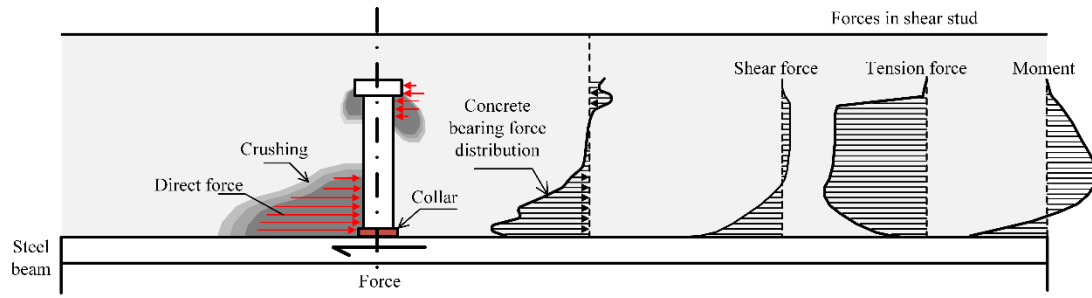
39  
40

d) Model SC-110Ur

41  
42

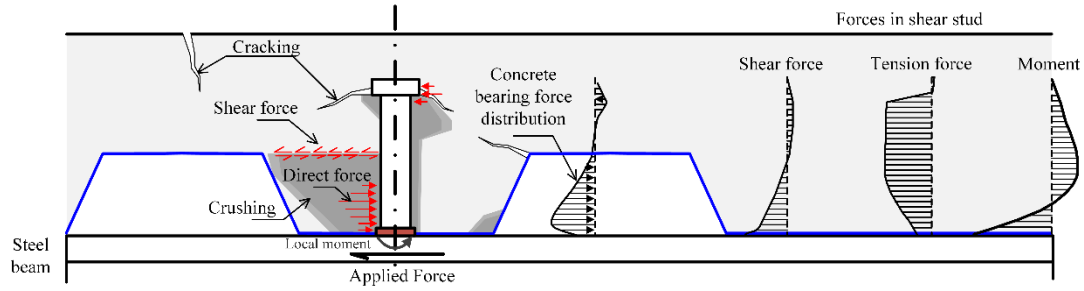
Figure 7 Distributions of damaged concrete in various models of shear connections

43



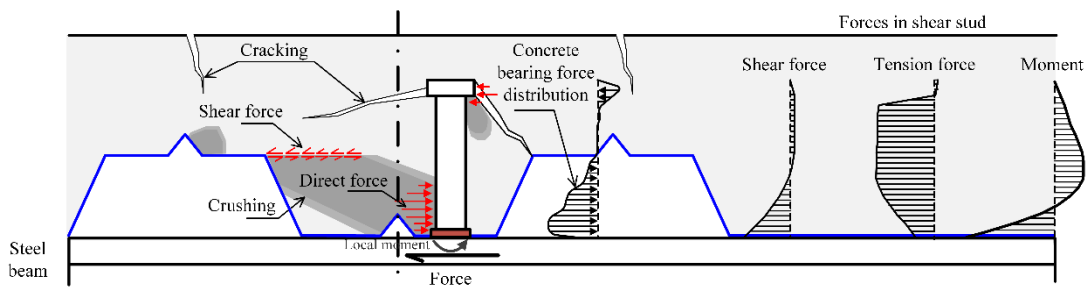
44  
45  
46  
47

a) Shear connection with a solid concrete slab: Model SS



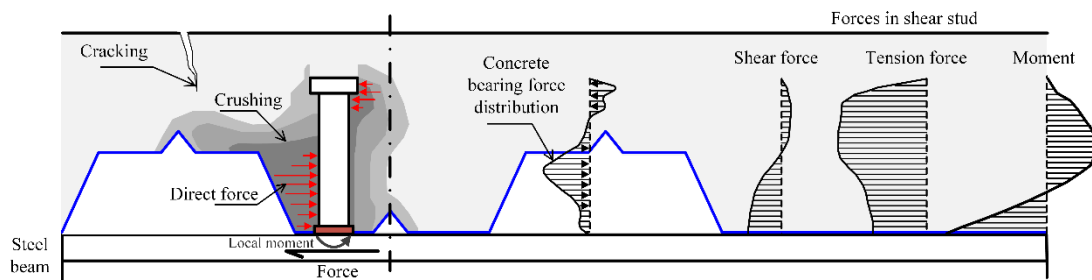
48  
49  
50  
51

b) Shear connection with a composite slab – Central position: Model SC



52  
53  
54  
55  
56

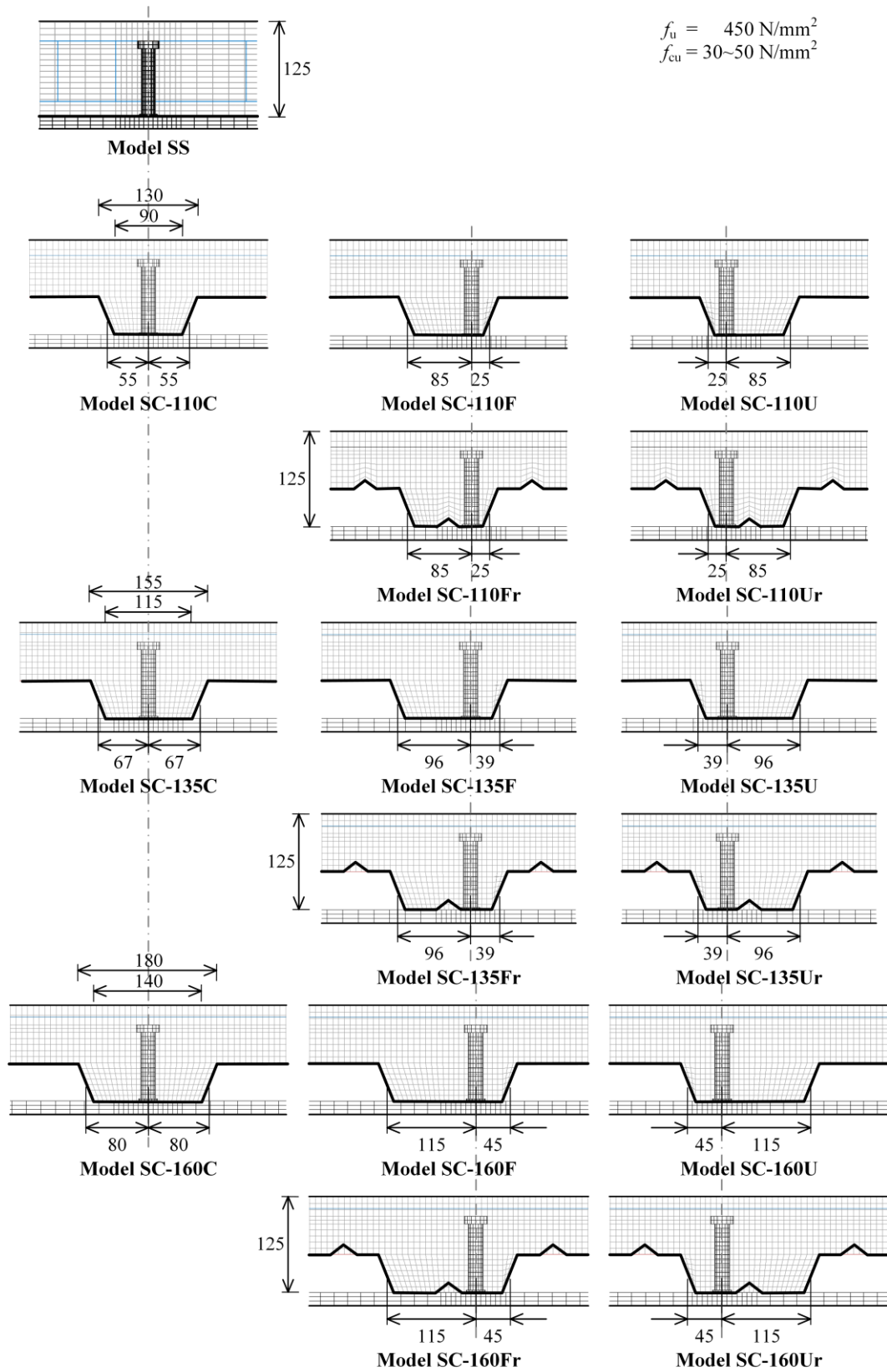
c) Shear connection with a composite slab – Favourable position: Model SCF



57  
58  
59  
60  
61

d) Shear connection with a composite slab – Unfavourable position: Model SCU

Figure 8 Load transfer mechanisms within various stud shear connections

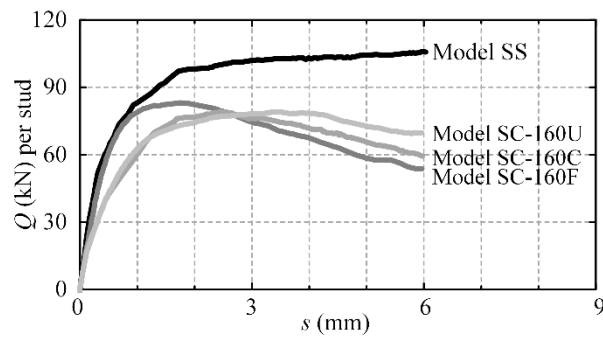


63  
64  
65

Figure 9: Finite element models of shear connections with various configurations

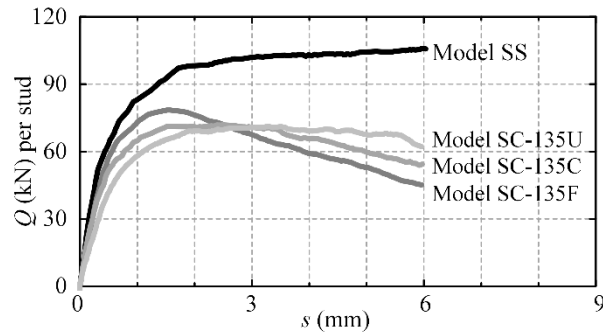


**Parametric study: PS01**



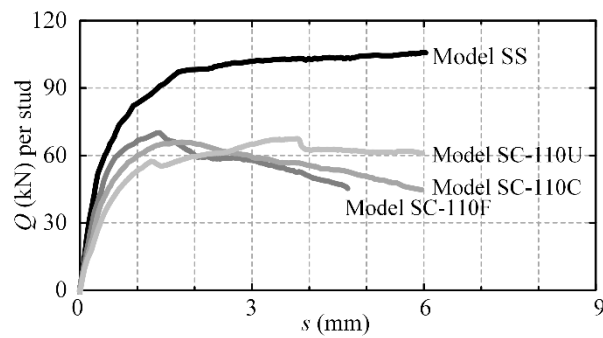
$b_o = 160 \text{ mm}$   
 $f_u = 450 \text{ N/mm}^2$   
 $f_{cu} = 30 \text{ N/mm}^2$

Models	$Q_m$ (kN)	$Q_m/Q_{SS}$	$s_m$ (mm)	$s_u$ (mm)	$s_m-s_u$ (mm)
SS	105.1	1.00	6.0	6.0	—
SC-160F	84.5	0.80	1.8	4.0	2.2
SC-160C	76.8	0.73	2.4	5.4	3.0
SC-160U	79.1	0.75	2.1	6.0	3.9



$b_o = 135 \text{ mm}$

Models	$Q_m$ (kN)	$Q_m/Q_{SS}$	$s_m$ (mm)	$s_u$ (mm)	$s_m-s_u$ (mm)
SS	105.1	1.00	6.0	6.0	—
SC-135F	78.5	0.75	1.5	3.6	2.1
SC-135C	72.2	0.69	2.0	5.2	3.2
SC-135U	71.7	0.68	2.0	6.0	4.0



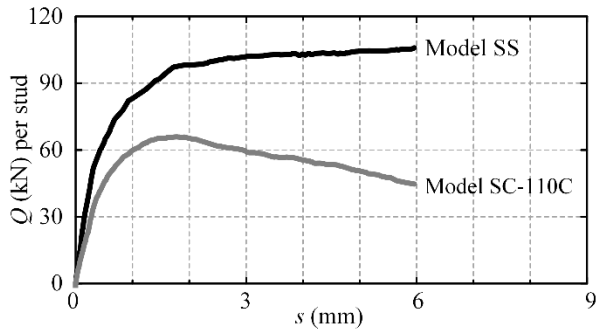
$b_o = 110 \text{ mm}$

Models	$Q_m$ (kN)	$Q_m/Q_{SS}$	$s_m$ (mm)	$s_u$ (mm)	$s_m-s_u$ (mm)
SS	105.1	1.00	6.0	6.0	—
SC-110F	68.5	0.65	1.4	3.3	1.9
SC-110C	65.5	0.62	1.8	5.0	3.2
SC-110U	65.3	0.62	1.8	6.0	4.2

66  
67  
68  
69  
70  
71  
72  
73

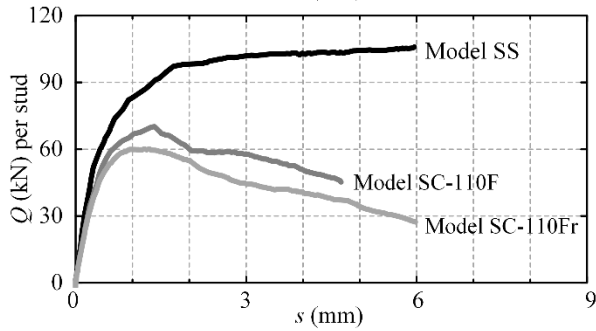
Figure 10: Deformation characteristics of shear connections with different installation positions and trough widths (Positions C, F and U for  $b_o = 110, 135$  and  $160 \text{ mm}$ )

**Parametric study: PS02a with  $b_o = 110$  mm**



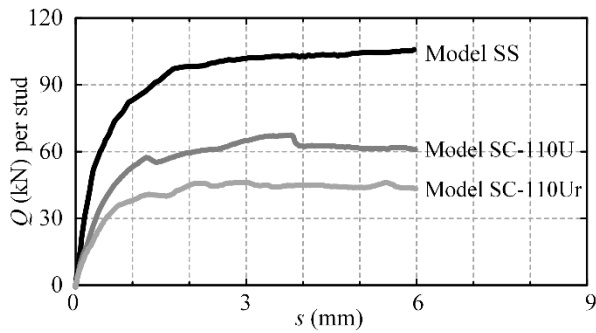
Central position

Models	$Q_m$ (kN)	$Q_m/Q_{SS}$	$s_m$ (mm)	$s_u$ (mm)	$s_u-s_m$ (mm)
SS	105.1	1.00	6.0	6.0	—
SC-110C	65.5	0.62	1.8	5.0	3.2



Favorable position

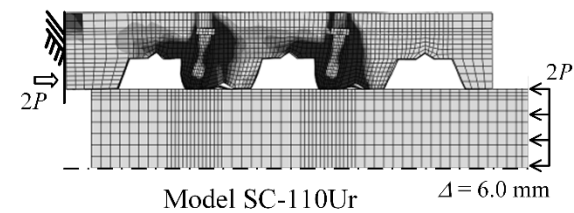
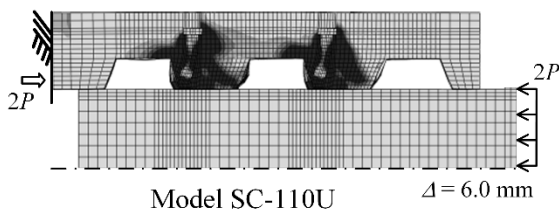
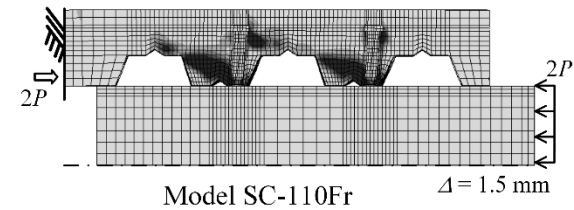
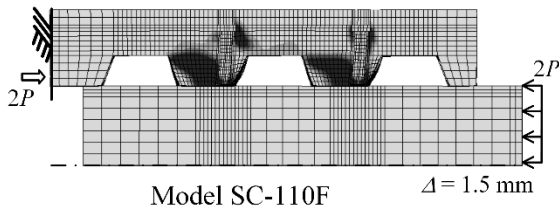
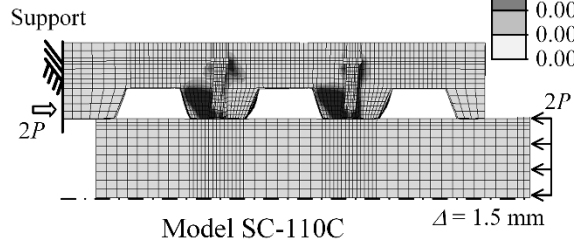
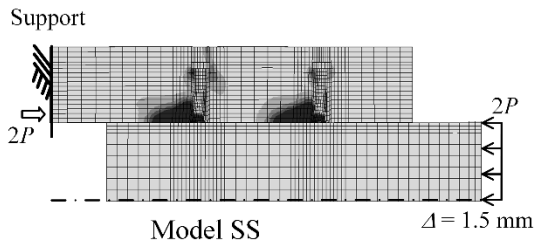
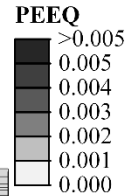
Models	$Q_m$ (kN)	$Q_m/Q_{SS}$	$s_m$ (mm)	$s_u$ (mm)	$s_u-s_m$ (mm)
SS	105.1	1.00	6.0	6.0	—
SC-110F	68.5	0.65	1.4	3.3	1.9
SC-110Fr	60.5	0.58	1.2	2.6	1.4



Unfavorable position

Models	$Q_m$ (kN)	$Q_m/Q_{SS}$	$s_m$ (mm)	$s_u$ (mm)	$s_u-s_m$ (mm)
SS	105.1	1.00	6.0	6.0	—
SC-110U	65.3	0.62	1.8	6.0	4.2
SC-110Ur	44.5	0.42	2.1	6.0	3.9

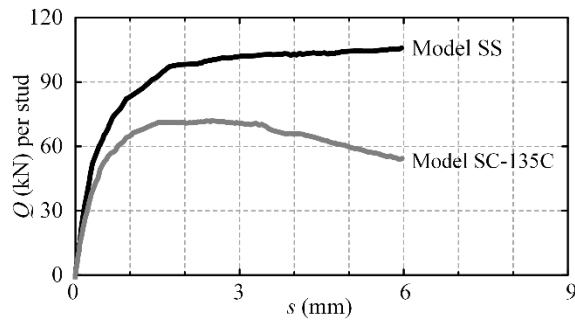
$f_u = 450 \text{ N/mm}^2$   
 $f_{cu} = 30 \text{ N/mm}^2$



74  
75  
76

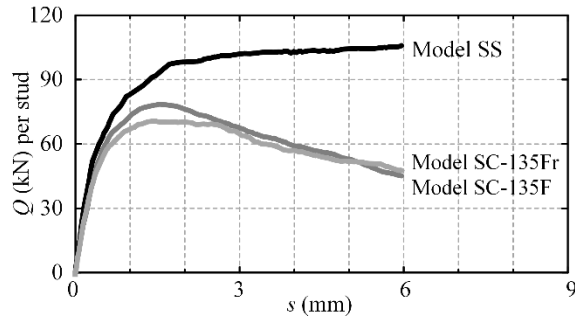
Figure 11: Numerical results of shear connections with different arrangements (Trough width  $b_o$  at 110 mm with various cases of Positions C, F & Fr, and U & Ur)

**Parametric study: PS02b with  $b_o = 135$  mm**



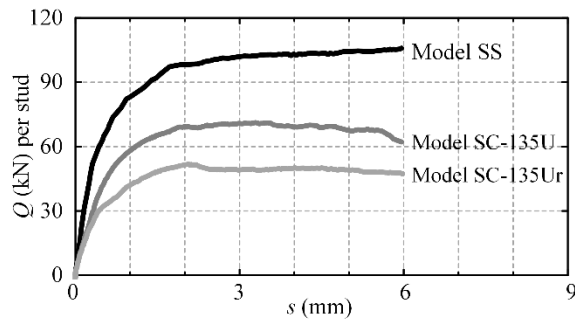
Central position

Models	$Q_m$ (kN)	$Q_m/Q_{SS}$	$s_m$ (mm)	$s_u$ (mm)	$s_u-s_m$ (mm)
SS	105.1	1.00	6.0	6.0	—
SC-135C	72.2	0.69	2.0	5.2	3.2



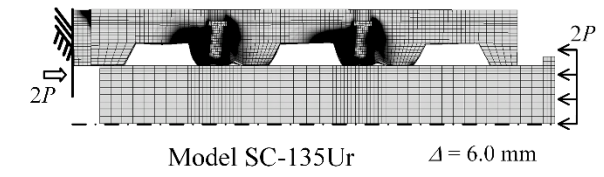
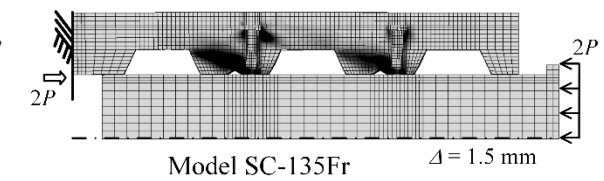
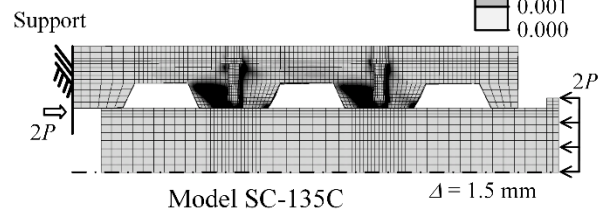
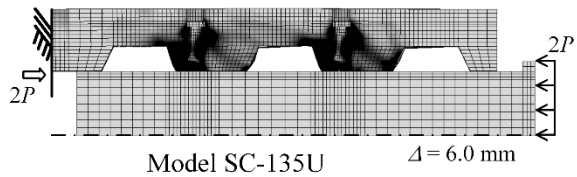
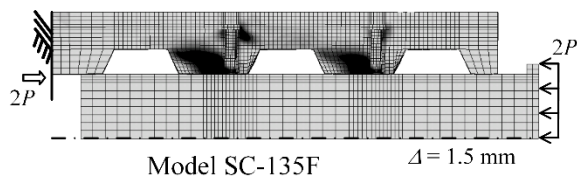
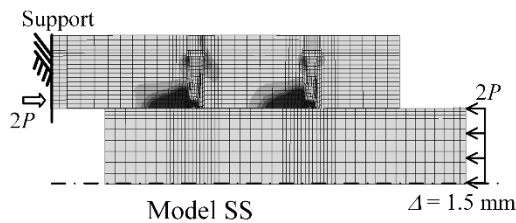
Favorable position

Models	$Q_m$ (kN)	$Q_m/Q_{SS}$	$s_m$ (mm)	$s_u$ (mm)	$s_u-s_m$ (mm)
SS	105.1	1.00	6.0	6.0	—
SC-135F	78.5	0.75	1.5	3.6	2.1
SC-135Fr	71.1	0.68	1.5	4.0	2.5



Unfavorable position

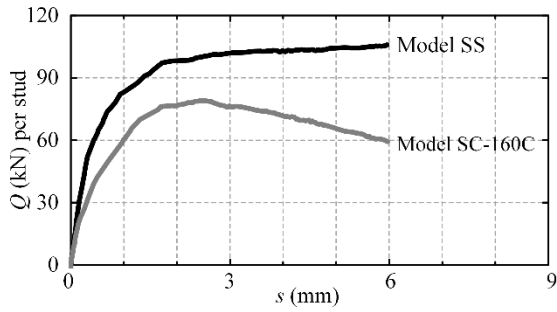
Models	$Q_m$ (kN)	$Q_m/Q_{SS}$	$s_m$ (mm)	$s_u$ (mm)	$s_u-s_m$ (mm)
SS	105.1	1.00	6.0	6.0	—
SC-135U	71.7	0.68	2.0	6.0	4.0
SC-135Ur	52.4	0.50	2.1	6.0	3.9



77  
78  
79  
80

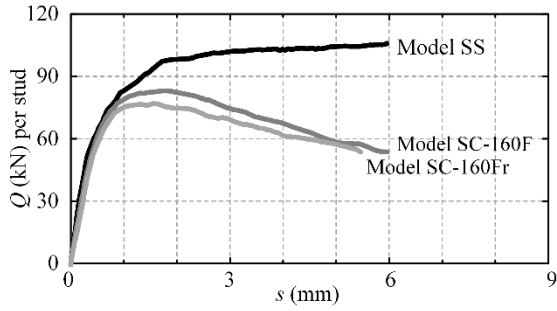
Figure 12: Numerical results of shear connections with different arrangements (Trough width  $b_o$  at 135 mm with various cases of Positions C, F & Fr, and U & Ur)

**Parametric study: PS02c with  $b_o = 160$  mm**



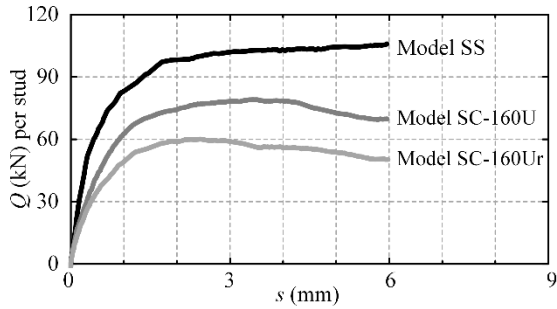
Central position

Models	$Q_m$ (kN)	$Q_m/Q_{SS}$	$s_m$ (mm)	$s_u$ (mm)	$s_u-s_m$ (mm)
SS	105.1	1.00	6.0	6.0	—
SC-160C	76.8	0.73	2.4	5.4	3.0



Favorable position

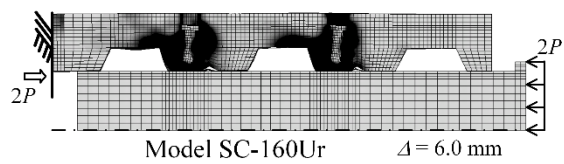
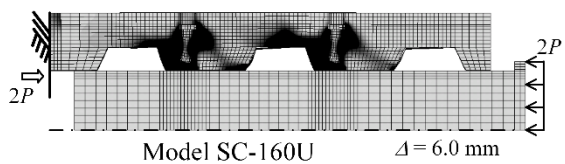
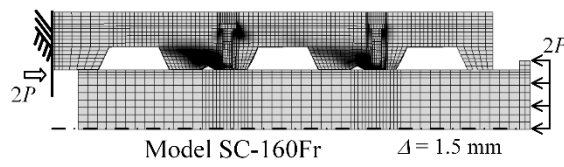
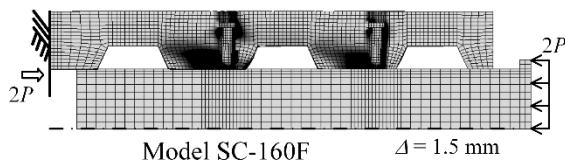
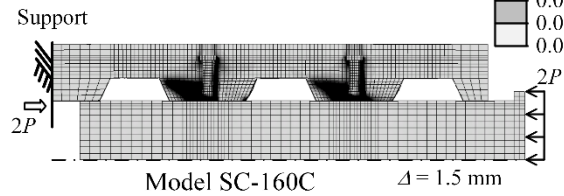
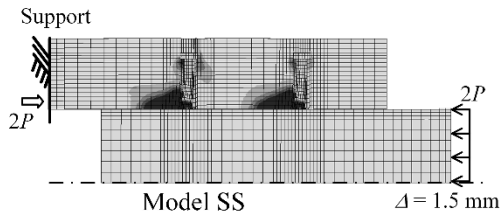
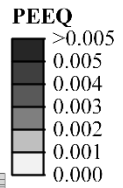
Models	$Q_m$ (kN)	$Q_m/Q_{SS}$	$s_m$ (mm)	$s_u$ (mm)	$s_u-s_m$ (mm)
SS	105.1	1.00	6.0	6.0	—
SC-160F	84.5	0.80	1.8	4.0	2.2
SC-160Fr	77.3	0.74	1.6	4.0	2.4



Unfavorable position

Models	$Q_m$ (kN)	$Q_m/Q_{SS}$	$s_m$ (mm)	$s_u$ (mm)	$s_u-s_m$ (mm)
SS	105.1	1.00	6.0	6.0	—
SC-160U	79.1	0.75	2.1	6.0	3.9
SC-160Ur	60.5	0.58	2.0	6.0	4.0

$f_u = 450 \text{ N/mm}^2$   
 $f_{cu} = 30 \text{ N/mm}^2$



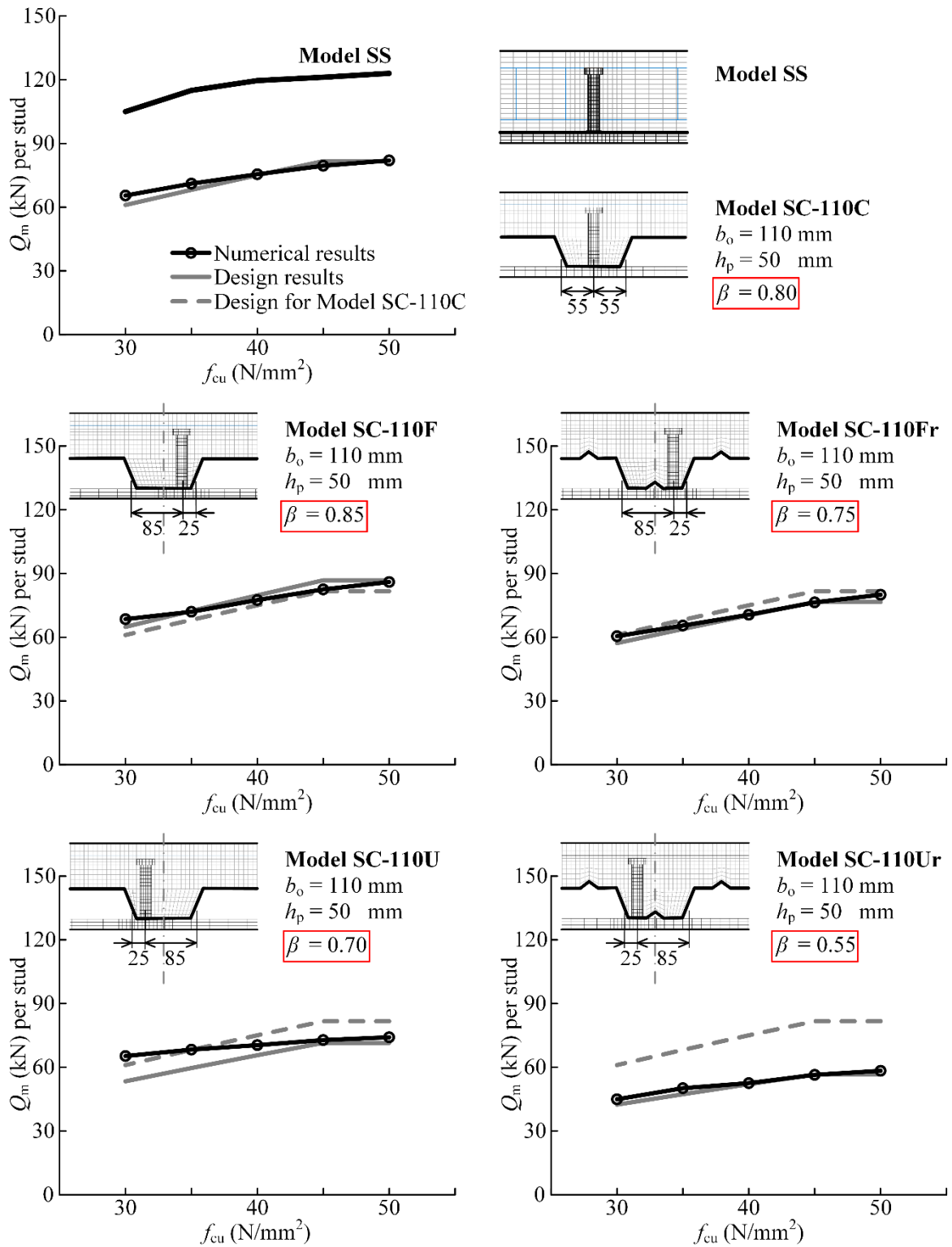
81

82

83

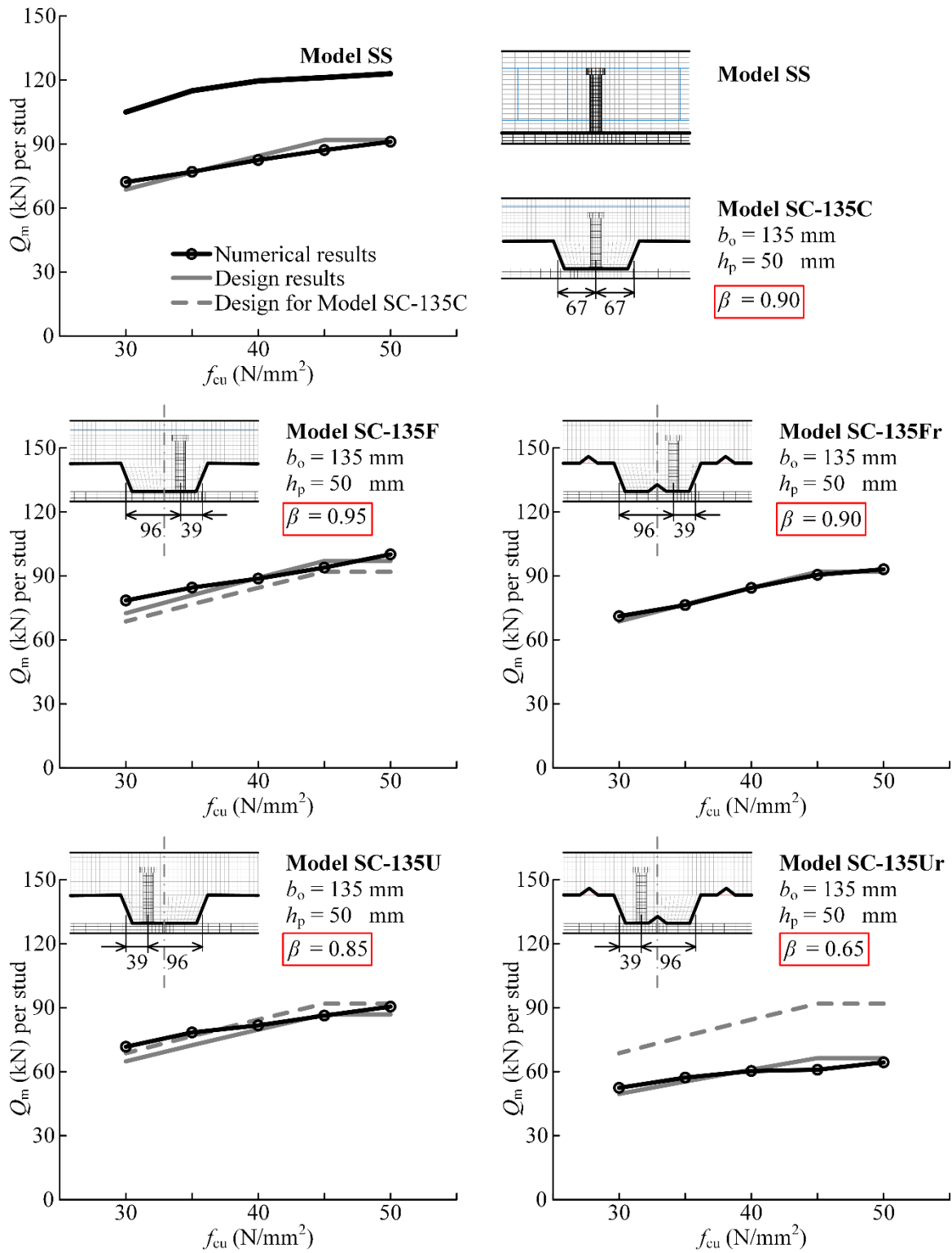
84

Figure 13: Numerical results of shear connections with different arrangements (Trough width  $b_o$  at 160 mm with various cases of Positions C, F & Fr, and U & Ur)



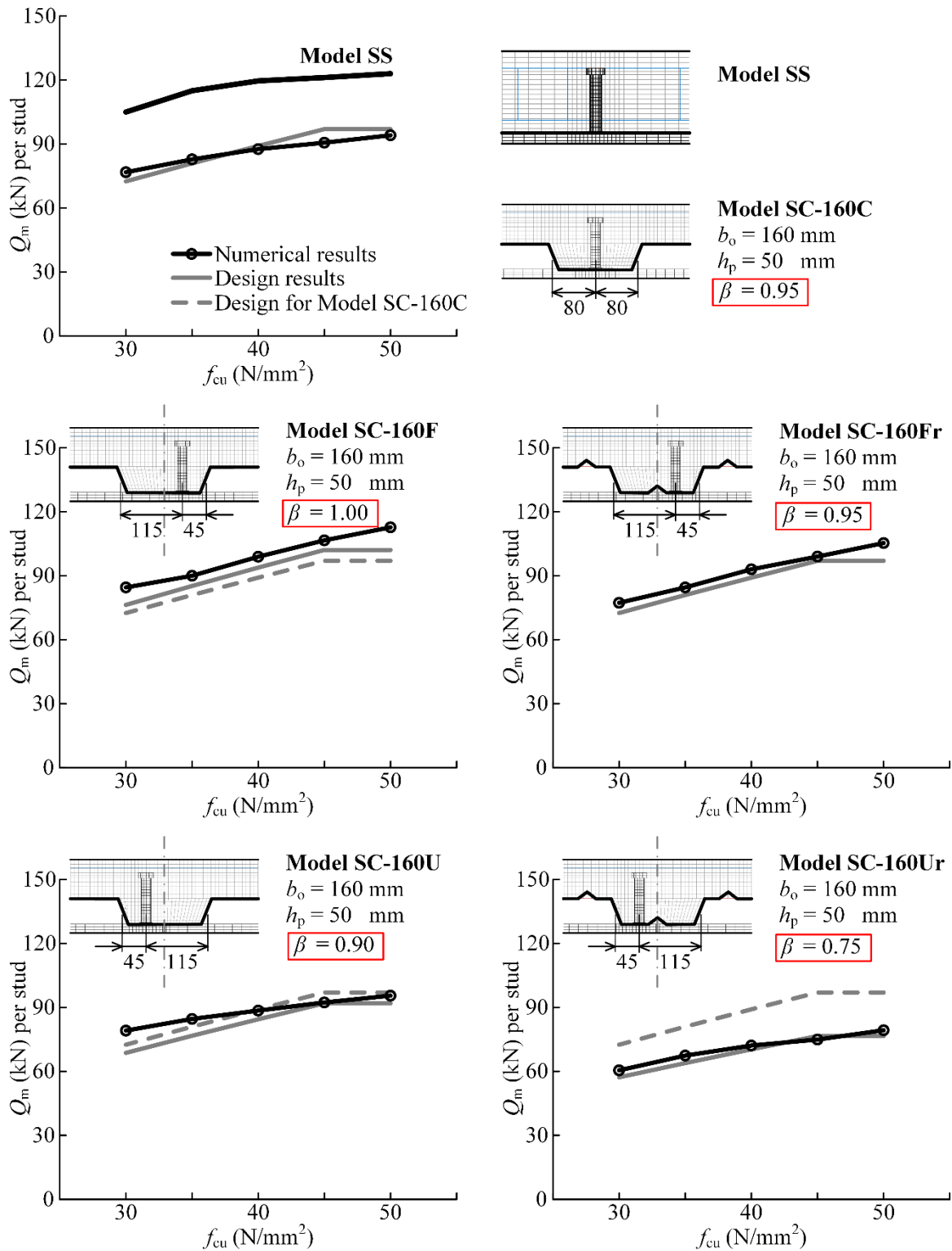
85  
 86  
 87  
 88

Figure 14: Shear resistances of stud shear connections with profiled decks:  
 Trough width  $b_o = 110$  mm



89  
 90  
 91  
 92  
 93

Figure 15: Shear resistances of stud shear connections with profiled decks:  
 Trough width  $b_o = 135$  mm



94  
 95  
 96  
 97  
 98  
 99

Figure 16: Shear resistance of stud shear connections with profiled decks:  
 Trough width  $b_o = 160$  mm

100

Table 1: Measured shear resistances and ductility limits

Test Series	$Q_m$ (kN)	$s_m$ (mm)	$Q_m/Q_{SS}$
SS	121.2	6.0	1.00
SCFr	58.9	1.2	0.52
SCUr	49.6	2.5	0.43

101

102

103

Table 2: Summary of convergence study of Series SS with different element sizes

104

a) Model SS with concrete of different element sizes

Finite element meshes	Shear resistance $Q_{FEM}$ (kN)	Relative resistance ratio	Computational time (hours)
C2-S2	120.0	1.026	0.5
C3-S2	117.6	1.005	2.7
C4-S2	117.0	1.000	21.5

105

106

b) Model SS with steel studs of different element sizes

Finite element meshes	Shear resistance $Q_{FEM}$ (kN)	Relative resistance ratio	Computational time (hours)
C3-S1	118.4	1.010	2.0
C3-S2	117.6	1.003	2.7
C3-S3	117.2	1.000	4.6

107

Note:  $Q_{FEM}$  is the predicted shear resistance of the shear connection at a slippage of 6.0 mm.

108

109

110

111

112

113

114

115



Table 3: Summary of parametric studies of stud shear connections

116  
117  
118

Study PS01

Installation position of headed shear studs	Central position	Favourable position	Unfavourable position
Composite slabs	<b>Model SC-160C</b>	<b>Model SC-160F</b>	<b>Model SC-160U</b>
	<b>Model SC-135C</b>	<b>Model SC-135F</b>	<b>Model SC-135U</b>
	<b>Model SC-110C</b>	<b>Model SC-110F</b>	<b>Model SC-110U</b>
Solid concrete slabs (reference)	Model SS		

119

120 Study PS02a:  $b_o = 110$  mm

Installation position of headed shear studs	Central position	Favourable position	Unfavourable position
Composite slabs	<b>Model SC-110C</b>	—	—
	—	<b>Model SC-110F</b>	<b>Model SC-110U</b>
	—	<b>Model SC-110Fr</b>	<b>Model SC-110Ur</b>

121

122 Study PS02b:  $b_o = 135$  mm

Installation position of headed shear studs	Central position	Favourable position	Unfavourable position
Composite slabs	<b>Model SC-135C</b>	—	—
	—	<b>Model SC-135F</b>	<b>Model SC-135U</b>
	—	<b>Model SC-135Fr</b>	<b>Model SC-135Ur</b>

123

124 Study PS02c:  $b_o = 160$  mm

Installation position of headed shear studs	Central position	Favourable position	Unfavourable position
Composite slabs	<b>Model SC-160C</b>	—	—
	—	<b>Model SC-160F</b>	<b>Model SC-160U</b>
	—	<b>Model SC-160Fr</b>	<b>Model SC-160Ur</b>

125

126

127

128

129  
130

Table 4: Configuration parameter  $\beta$

Trough width $b_o$ (mm)	Installation positions of the shear studs				
	C	F	Fr	U	Ur
110	0.80	0.85	0.75	0.70	0.55
135	0.90	0.95	0.90	0.85	0.65
160	0.95	1.00	0.95	0.90	0.75

Notes:

- “C” indicates a shear stud installed in central position of a decking trough;
- “F” indicates a shear stud installed in a favourable position of a decking trough;
- “U” indicates a shear stud installed in unfavourable position of a decking trough; and
- “r” indicates presence of longitudinal stiffeners in the central position of a decking trough.

131